3 Immune response to *C. rodentium* in miR-155-deficient mice

3.1 Introduction

Infection of C57BL/6 mice with the bacterial pathogen *C. rodentium* can result in colonic mucosal hyperplasia and a local T_h1 inflammatory response characterised by increased transcription of type 1 cytokines such as IL-12, TNF-α, and IFN-γ. Bacterial colonisation is associated with the colonic mucosa, and normal wild-type adult mice clear the infection spontaneously within ~21-28 days pi. Studies in mice with targeted deletions of the immune system have helped to identify a number of immune factors involved in control of *C. rodentium* infection. In particular, the adaptive immune system, including T and B cells, has been shown to play an essential role in containing and eradicating the infection.

miR-155 has recently been implicated as an important player in both the innate and adaptive immune systems. Previous studies have shown that miR-155 is expressed in a variety of activated immune cells. Specifically, miR-155 is rapidly expressed in $CD4^+$ T cells and macrophages following activation with bacterially and virally relevant stimuli and consequently enhances the production of TNF-α. Furthermore, miR-155-deficient mice show reduced B cell-associated humoral responses. However, most studies have focused on the critical role of miR-155 in isolated immune cells, and thus the role of miR-155 in the context of the overall immune response during active infection still remains to be elucidated.

3.2 Results

3.2.1 miR-155 expression in C57BL/6 mice following infection with *C. rodentium*

To identify whether miR-155 is induced during a mucosal infection, we orally infected wild-type C57BL/6 mice with 10^9 organisms of *C. rodentium* and the

expression of miR-155 in colonic tissue was monitored at various time-points pi, using RT-PCR. The colonisation and clearance of *C. rodentium* was simultaneously measured throughout infection by assessing viable counts recovered from stools. Shedding of *C. rodentium* during this period followed the classical growth curve reported previously[171]. Briefly, *C. rodentium* levels in the colon peaked on day 4 after infection and remained high (~10^7 CFU/g faeces) for approximately a week. Following day 12 pi, bacterial levels began to decline until complete clearance had been achieved by day 23 pi. Time course studies demonstrated that transcription of miR-155 is significantly induced in colonic tissue by *C. rodentium* infection (Figure 28). Additionally, we observed that miR-155 expression is closely associated with the burden of colonic *C. rodentium*. In mice orally infected with *C. rodentium*, miR-155 transcripts rapidly increased following infection, peaked on day 4 pi when colonisation in the colon is at its highest and subsequently fell as bacterial numbers decayed. Upon clearance of *C. rodentium*, the expression of miR-155 returned to pre-infection levels.

However, it should be noted that the single biggest limitation of this study is that, expression data at each of the time points assayed is based on sampling from two mice. Consequently, such a sample size may be too small to provide robust results and additionally could be a major contributing factor to the variation observed in miR-155 expression, particularly as miR-155 expression declines. Such experiments are expensive and labour intensive so to date we have been unable to repeat this experiment.

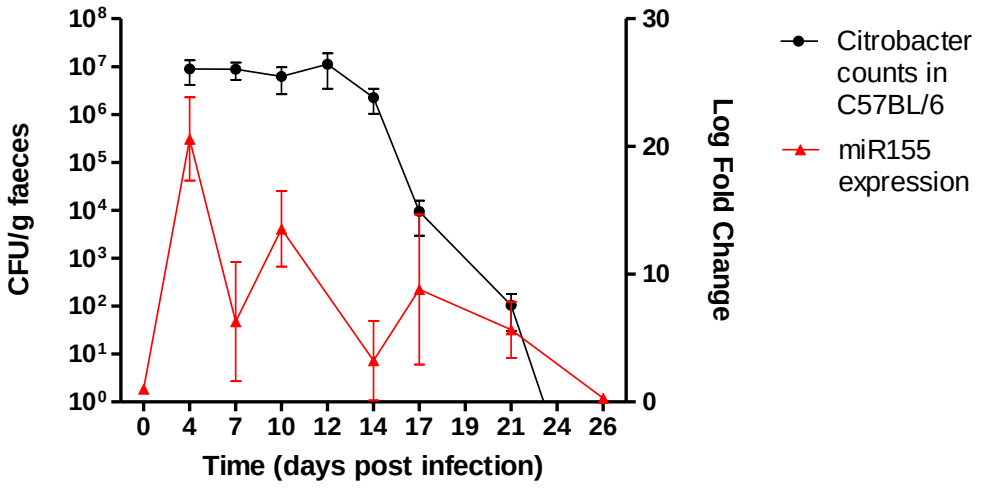

Figure 28. Expression of *miR-155* gene in C57BL/6 mice infected with *C. rodentium*.

C57BL/6 mice were orally infected with 10^9 organisms of *C. rodentium*. The colonisation and clearance of *C. rodentium* was measured throughout infection by assessing viable counts recovered from faecal samples at 4, 7, 10, 12, 14, 17, 19, 21 and 23 days after inoculation (black line), (±SEM), n=7 mice. Total miRNAs were extracted from colonic tissues of mice orally infected with *C. rodentium*. The expression of miR-155 at various time-points pi was monitored by RT-PCR (red line). Data depicts the mean Log fold change (± SEM) of miR-155 transcripts, n=2 mice per time point.

3.2.2 Prolonged clearance of *C. rodentium* infection in miR-155-deficient mice

Given that miR-155 is significantly induced by *C. rodentium* infection we wished to ascertain the impact of the loss of miR-155 on pathogenesis. To this end, we used a genetic approach to determine if miR-155 contributes to immunity to *C. rodentium* by employing mice with targeted deletions of the miR-155 gene[31]. miR-155-deficient and control C57BL/6 mice were orally infected with *C. rodentium* and the numbers of CFUs in faecal samples were determined as an indication of the extent of colonisation. We found that during the early to middle phases of infection, days 4-14 after challenge, there were no obviously significant differences in faecal CFU between miR-155-deficient and control mice (Figure 29a). However, after day 14, whilst control mice began to clear infection, miR-155-deficient mice remained chronically infected and displayed significantly greater bacterial loads (Figure 29a). By day 20, all C57BL/6 mice had resolved infection. This was in stark contrast to miR-155-deficient mice which took on average 20 additional days to achieve complete clearance, P value < 0.0001 (Figure 29b). It is worth noting that during infection there were no obvious disease related mortalities amongst either group and, all miR-155-deficient mice eventually successfully resolved infection.

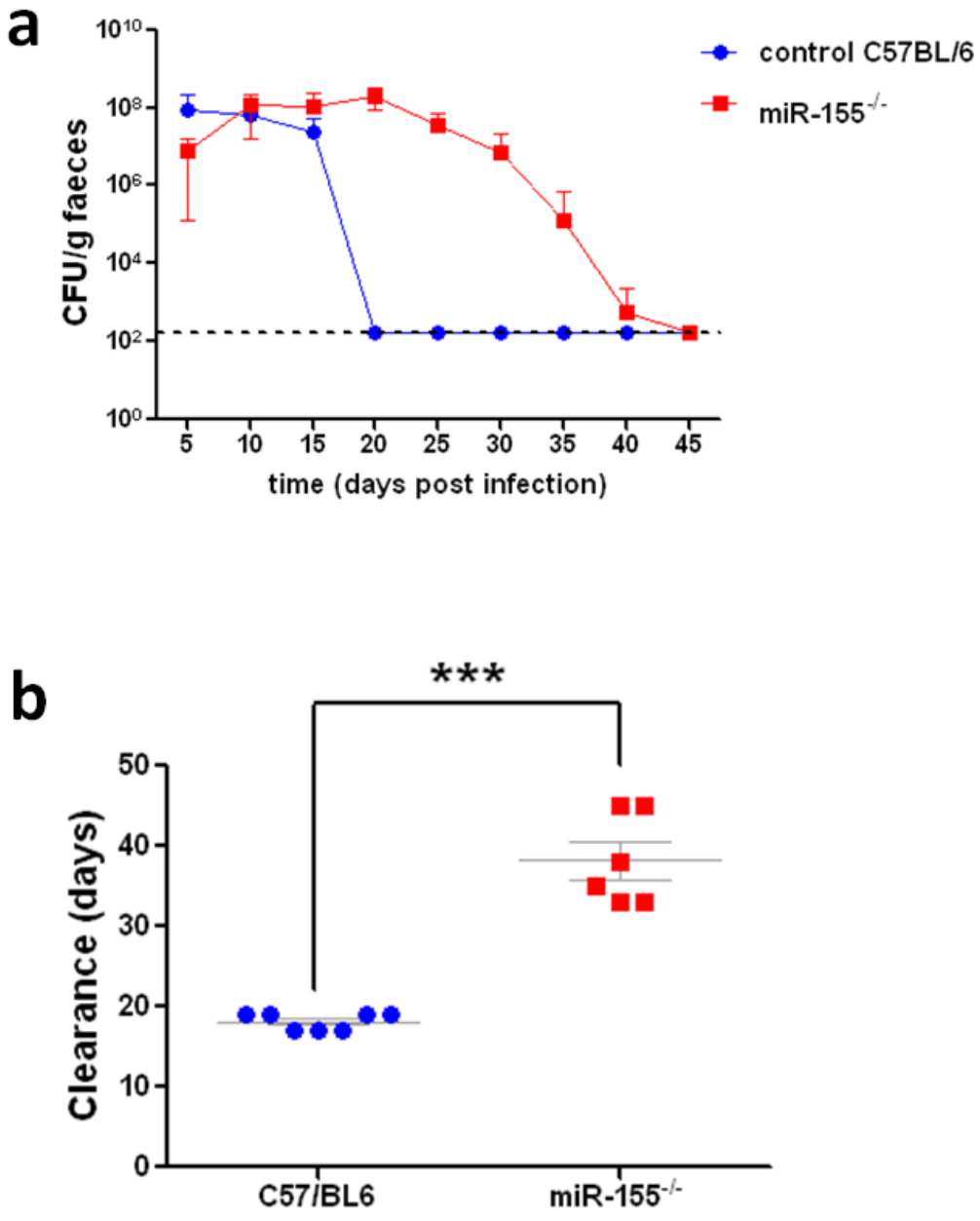

Figure 29. Colonisation and clearance of *C. rodentium* in miR-155-deficient and C57BL/6 mice

Susceptibility to *C. rodentium* infection in miR-155-deficient (miR-155$^{-/-}$) mice. miR-155-deficient and control C57BL/6 mice were orally gavaged with approximately 1x10^{9} CFU of *C. rodentium*. (a) Viable *C. rodentium* were enumerated from faecal samples by plating on LB agar supplemented with naladixic acid, n=7 C57BL/6 and n=6 miR-155-deficient mice. (b) Time (days) taken to resolve infection (± SEM), *** indicates P value <0.0001 by Student's t-test.

3.2.3 Increased *C. rodentium* pathogen burden in gastrointestinal tissues of miR-155-deficient mice

To establish whether the prolonged clearance time observed in miR-155-deificent mice was associated with increased pathogen burden within infected tissues, miR-155-deficient and control C57BL/6 mice were orally infected with 10^9 CFU of *C. rodentium* and the numbers of CFUs in gastrointestinal tissues were determined at various time points pi.

miR-155-deficient mice demonstrated gastrointestinal burdens of *C. rodentium* similar to those seen in control mice during the initial stages of infection. At days 4 and 14 pi, bacterial burden in the colon, caecal patch and caecal contents of miR-155-deficient mice were not significantly different from those observed in controls (Figure 30). However, whilst pathogen burdens in C57BL/6 had fallen considerably by day 20 pi, the burden in miR-155-deficient mice was persistent (Figure 31). Additionally, on day 20 pi, miR-155-deficient mice had significantly greater numbers of bacteria in the caecum than in similarly infected C57BL/6 mice (Figure 31b). Furthermore, 26 days after infection, we were still able to isolate viable *C. rodentium* from the gastrointestinal tissues taken from miR-155-deficient mice, but not those from C57BL/6 mice (Figure 31c).

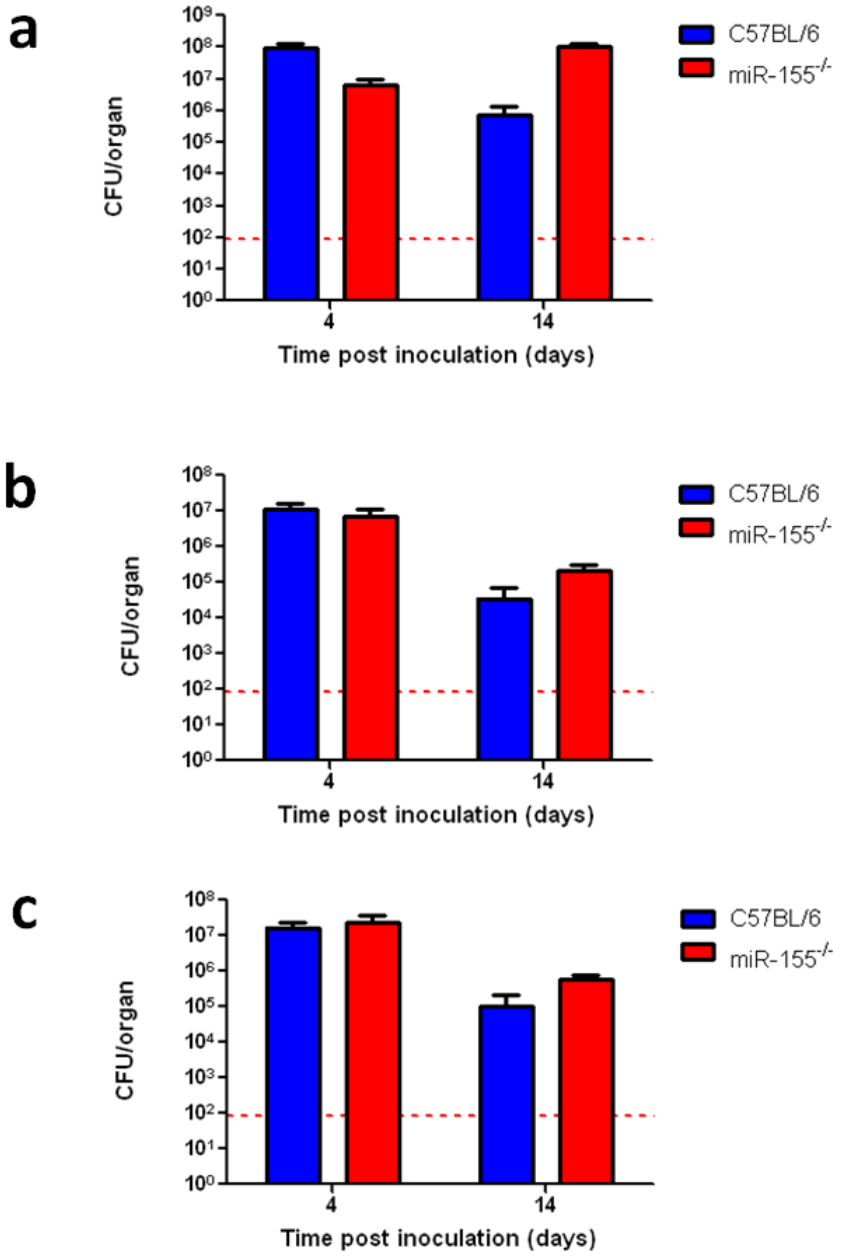

Figure 30. *C. rodentium* burden in gastrointestinal tissues of C57BL/6 and miR-155-deficient mice on day 4 and 14 pi.

Control C57BL/6 (blue bars) and miR-155-deficient (red bars) mice were orally infected with 10^9 organisms of *C. rodentium.* On days 4 and 14 pi, mice were sacrificed and numbers of *C. rodentium* (±SEM) in gastrointestinal tissue; (a) colon, (b) caecum and (c) caecal patch were enumerated, n=5 mice per group. Red broken lines indicate the detection level of the assay.

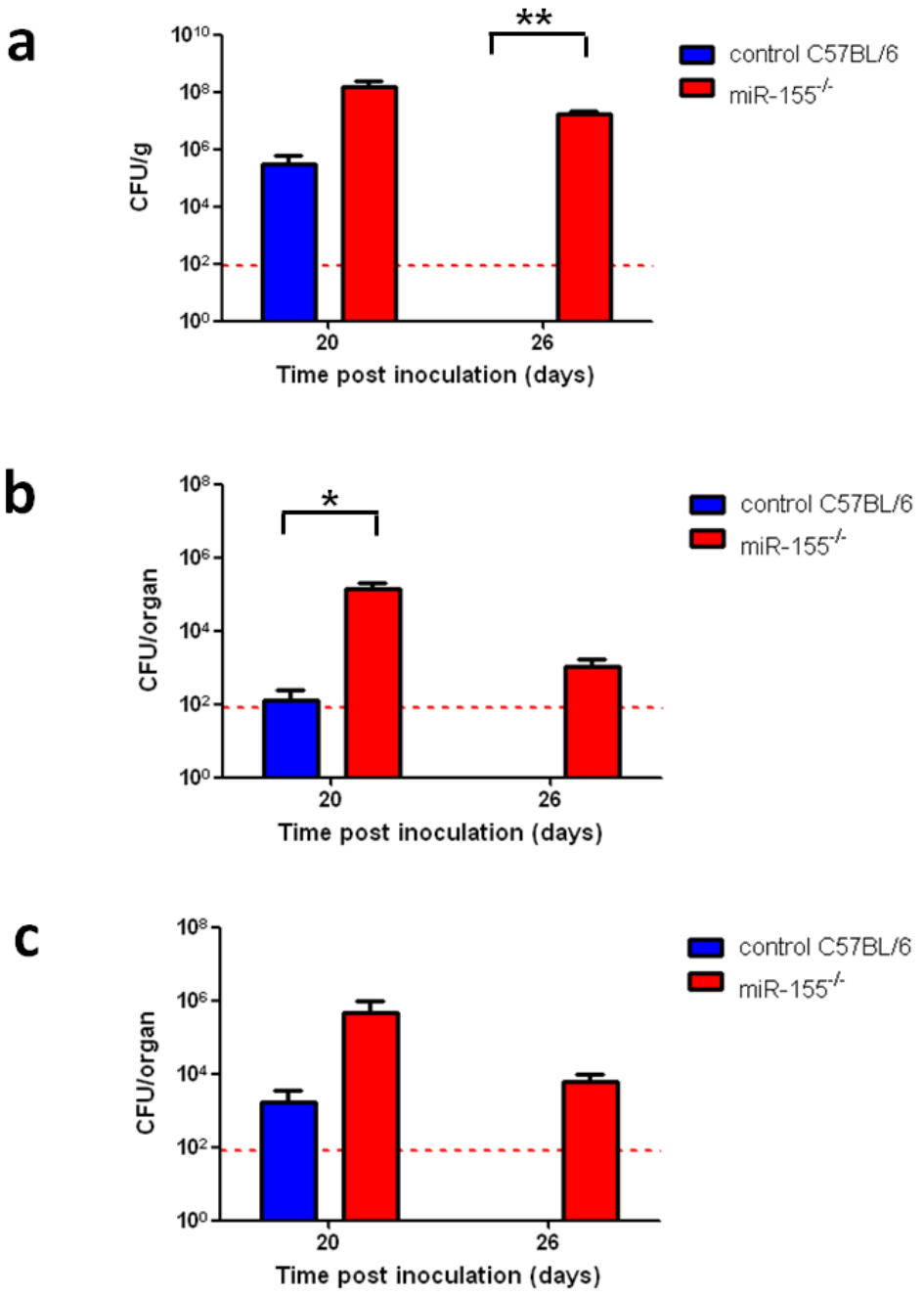

Figure 31. *C. rodentium* burden in gastrointestinal tissues of C57BL/6 and miR-155-deficient mice on day 20 and 26 pi

Control C57BL/6 (blue bars) and miR-155-deficient (red bars) mice were orally infected with 10^9 organisms of *C. rodentium.* On days 20 and 26 pi, mice were sacrificed and numbers of *C. rodentium* (±SEM) in gastrointestinal tissue; (a) colon, (b) caecum and (c) ceacal patch were enumerated, n=5 mice per group, ** indicates P value <0.0027 and * indicates P value <0.0353 by students t test. Red broken lines indicate the detection level of the assay.

3.2.4 miR-155-deficient mice develop more severe pathological changes in the colonic mucosa

C57BL/6 mice infected with *C. rodentium* characteristically develop colonic hyperplasia concurrently with peak pathogen burden in the colon, as indicated by significant proliferation of the colonic epithelia, crypt hyperplasia and dilation and thickening of the colonic mucosa. Analysis of distal colons from infected mice revealed that miR-155-deficient mice develop more severe *C. rodentium*-induced colonic hyperplasia than control C57BL/6 mice. From 14 days after infection the distal colons of infected miR-155-deficient mice were visibly thickened and weighed significantly more than colons of infected C57BL/6 mice (Figure 32a, b and c). Histological analysis of colonic tissue from infected miR-155-deficient mice revealed grossly elongated colonic crypts and polymorphonuclear infiltrate in the lamina propria and submucosa (Figure 32d, e and f).

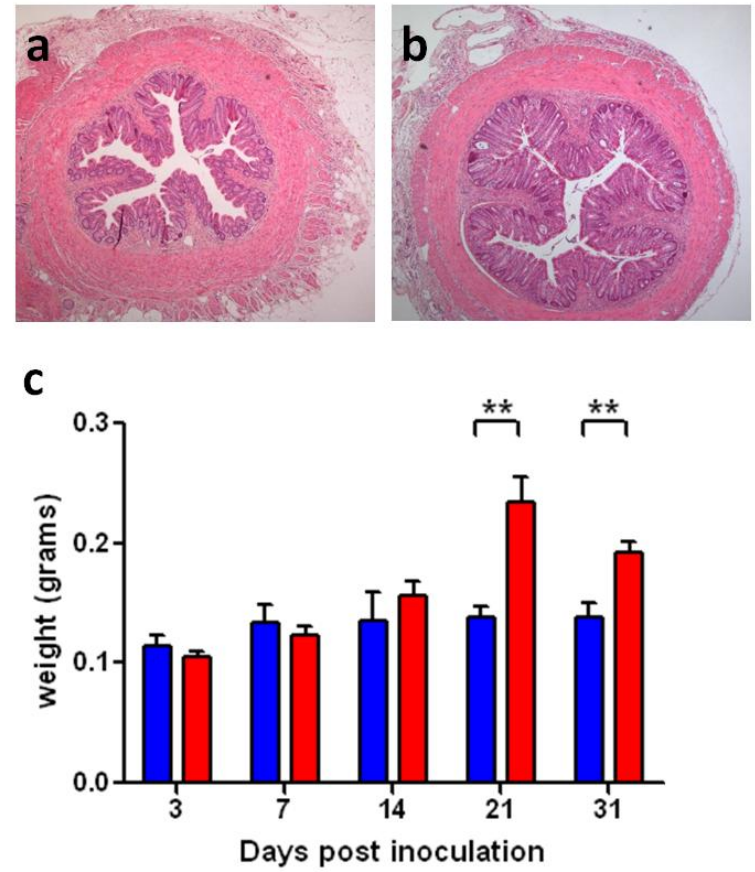
a
b
c
**
**
0.3
0.2
0.1
0.0
weight (grams)
3
7
14
21
31
Days post inoculation
d
e
f
***
250
200
150
100
50
0
Average crypt length (µm)
WT
miR-155-/-

Figure 32. Histopathological analysis of infected colons from miR-155-deficient and control C57BL/6 mice

Histopathological analyses (haematoxylin and eosin-stained sections; original magnification, x5) of colon sections from control C57BL/6 (a) and miR-155-deficient mice (b) on day 14 pi, images are representative of 5 mice per group. The distal colon of infected miR-155-deficient mice weighed significantly more than the colons of infected C57BL/6 mice at 21 and 31 days pi, n=4 mice per group, ** indicates P value <0.0052 and <0.0091 respectively (c). The panels (toluidine blue-stained sections; original magnification x40) show representative stained colonic sections from infected C57BL/6 (d) and miR-155-deficient mice (e) on day 14 pi. Colonic crypts in infected miR-155-deficient mice were significantly elongated (f) Average crypt length (±SEM) was determined from colon sections, n=5 mice per group, *** indicates P value <0.0001 by students t test.

3.2.5 Deficiency of miR-155 leads to the development of polymicrobial infections and severe damage to the colonic mucosa

Closer examination of colons from infected mice using histochemistry and electron microscopy revealed that while the colonic epithelium remained grossly intact in wild-type, knockout mice demonstrated more severe destruction of the epithelium of the distal colon. On day 14 pi, whilst control C57BL/6 mice showed relatively few remaining bacteria present on the epithelial surface and only minor damage to the colonic epithelium, miR-155-deficient mice displayed areas still heavily colonised by bacteria and considerable damage to luminal colonocytes (Figure 33a, c, d and f). Additionally, in miR-155-deficient mice, we observed frequent breaks in the epithelium integrity through which neutrophils and other polymorphonuclear cells had leaked into the lumen (Figure 33b and e).

Unusually, in amongst the areas that remained densely colonised, we noted the presence of microcolonies of cocci intimately adhered to the epithelial surface in miR-155-deficient mice but not controls (Figure 34). This is suggestive that infection with *C. rodentium* in miR-155-deficient mice may lead to a polymicrobial infection, perhaps involving association with components of the microbial flora with the epithelial surface. 16S ribosomal DNA sequence analysis would allow us to accurately identify spatial and temporal changes in the gut microbiome of miR-155-deficient and control mice during infection with *C. rodentium* and we are currently undertaking this analysis[206, 207].

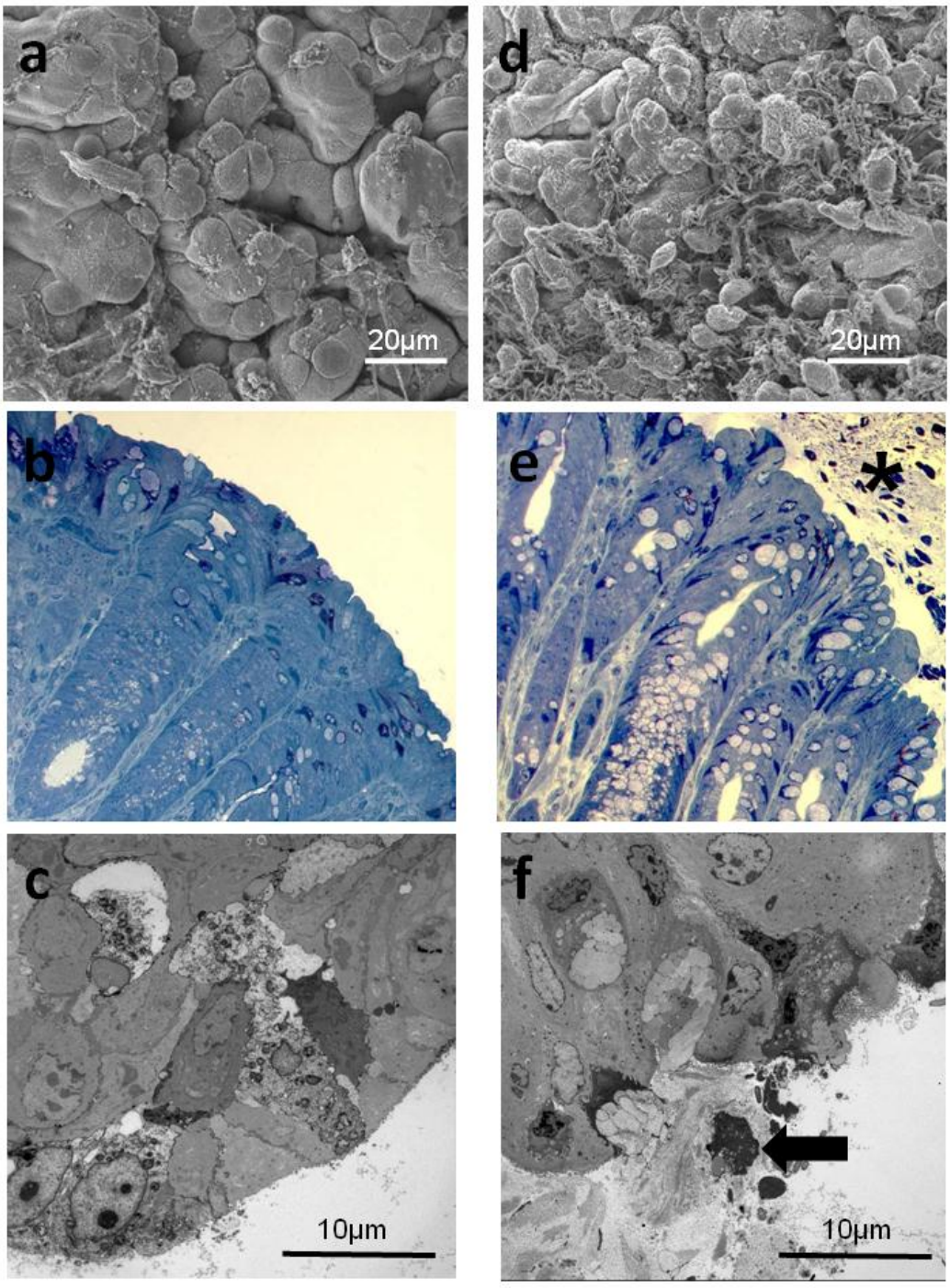

Figure 33. Histopathology in the distal colon of infected C57BL/6 and miR-155$^{-/-}$ mice

Colonic pathology observed at day 14 pi with *C. rodentium*. Colonic epithelium from C57BL/6 (a) and miR-155-deficient mice (d) was examined by scanning electron microscopy (SEM). Micrograph from a C57BL/6 mouse showing relatively few remaining bacteria present on the epithelial surface and only minor damage (a) whilst miR-155-deficient demonstrate heavy bacterial colonisation and considerable damage to luminal colonocytes.

Toluidine blue staining, magnification x200 (b and e) and transmission electron microscopy (c and f) of colonic mucosa from C57BL/6 and miR-155-deficient mice, respectively, at 14 days pi. C57BL/6 mouse, demonstrating a grossly intact colonic epithelium (b and c). miR-155-deficient mouse showing considerably more severe destruction of the epithelium and breaks through which neutrophils have entered the lumen (asterisk and arrow) (e and f).

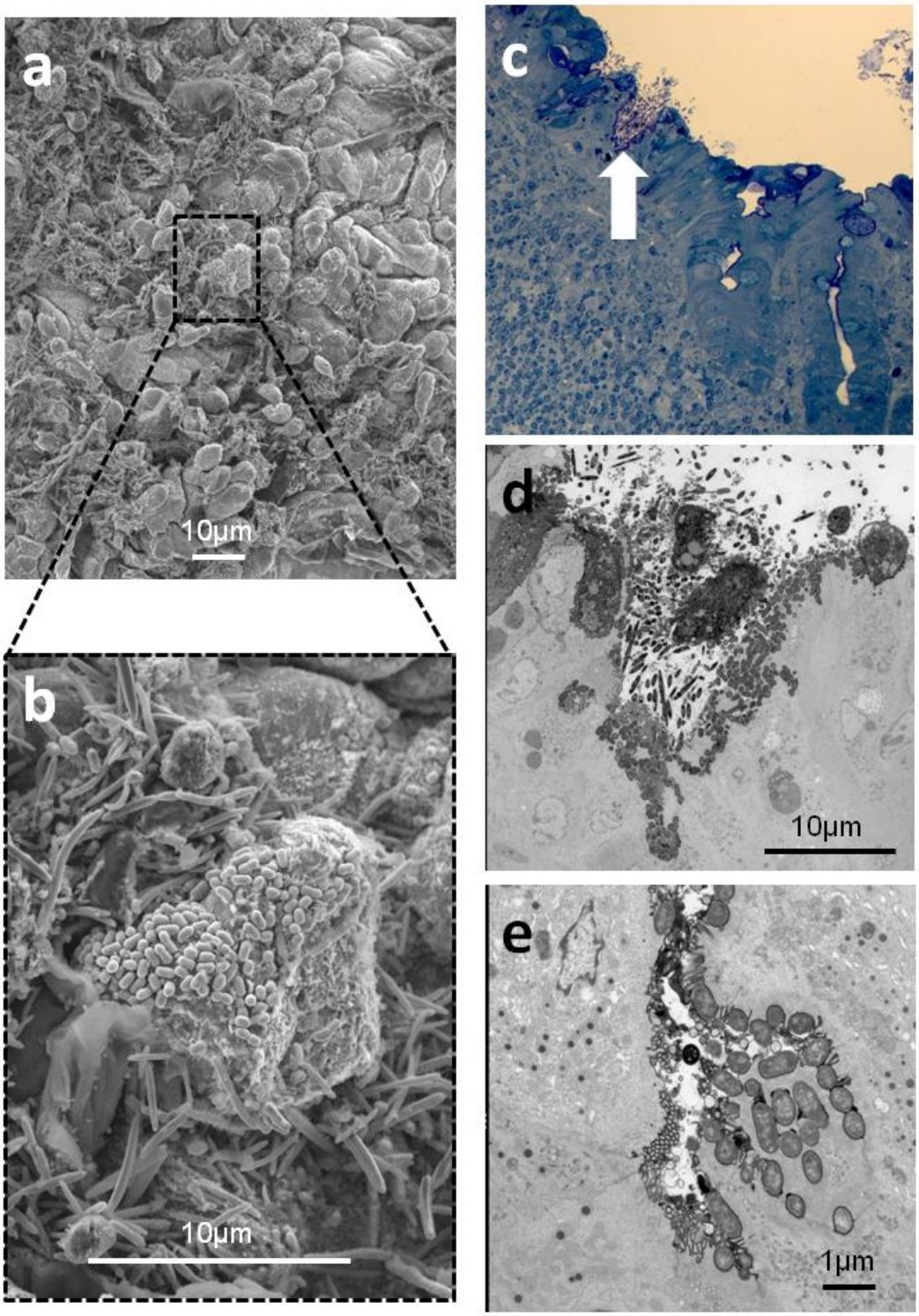

Figure 34. Polymicrobial infection in miR-155-deficient mice infected with *C. rodentium*.

Scanning electron microscopy (a and b), toluidine blue staining, magnification x40 (c), and transmission electron microscopy (d and e) of polymicrobial colonies observed in colonic

epithelium from miR-155-deficient mice 14 days after infection with *C. rodentium*. Amongst the areas heavily colonised by *C. rodentium* we observed numerous isolated dense microcolonies of cocci intimately attached to the epithelial surface (a and b). Arrow points to a crypt heavily colonised with *C. rodentium* and unidentified cocci (c). Dead and/ or severely damaged infected colonocytes are exfoliated into the lumen (d). Cocci intimately attached to luminal colonocytes, causing localized destruction of the brush-border microvilli and beginning to penetrate through the epithelial barrier into the lamina propria beneath (e).

3.2.6 Systemic spread of *C. rodentium* in miR-155-deficient mice

During the peak of infection, bacterial numbers in the colon can exceed 10^9 organisms per gram of tissue, a significant pathogen burden[161, 164-166]. However, despite the extremely high levels of colonisation the colonic epithelium remains grossly intact, with rare breaks occurring only occasionally as a result of abscess formation and subsequent efflux of neutrophils into the lumen[170]. Such breaks provide portals through which *C. rodentium* and resident gut flora may disseminate to systemic sites[170, 208]. Given that miR-155-deficient mice display more severe colonic damage and frequent epithelial breaks during infection with *C. rodentium*, we wished to investigate if bacteria are able to traverse the damaged epithelia and disseminate to distant sites resulting in a systemic infection.

miR-155-deficient and C57BL/6 mice were infected with *C. rodentium* and systemic tissues were collected on days 20 and 26 pi, and the pathogen burden was determined by viable count. No CFU were cultured from internal organs of C57BL/6 mice at either time point assayed (Figure 35). Unlike C57BL/6 mice, several miR-155-deficient mice exhibited considerable numbers (~10^3 CFU/organ) of *C. rodentium* in the spleen, liver and mLNs on day 20 pi, thus providing evidence of systemic infection (Figure 35). Additionally, 26 days after infection, 25% of miR-155-deficient mice still had significantly greater pathogen burdens in the spleen (Figure 35b).

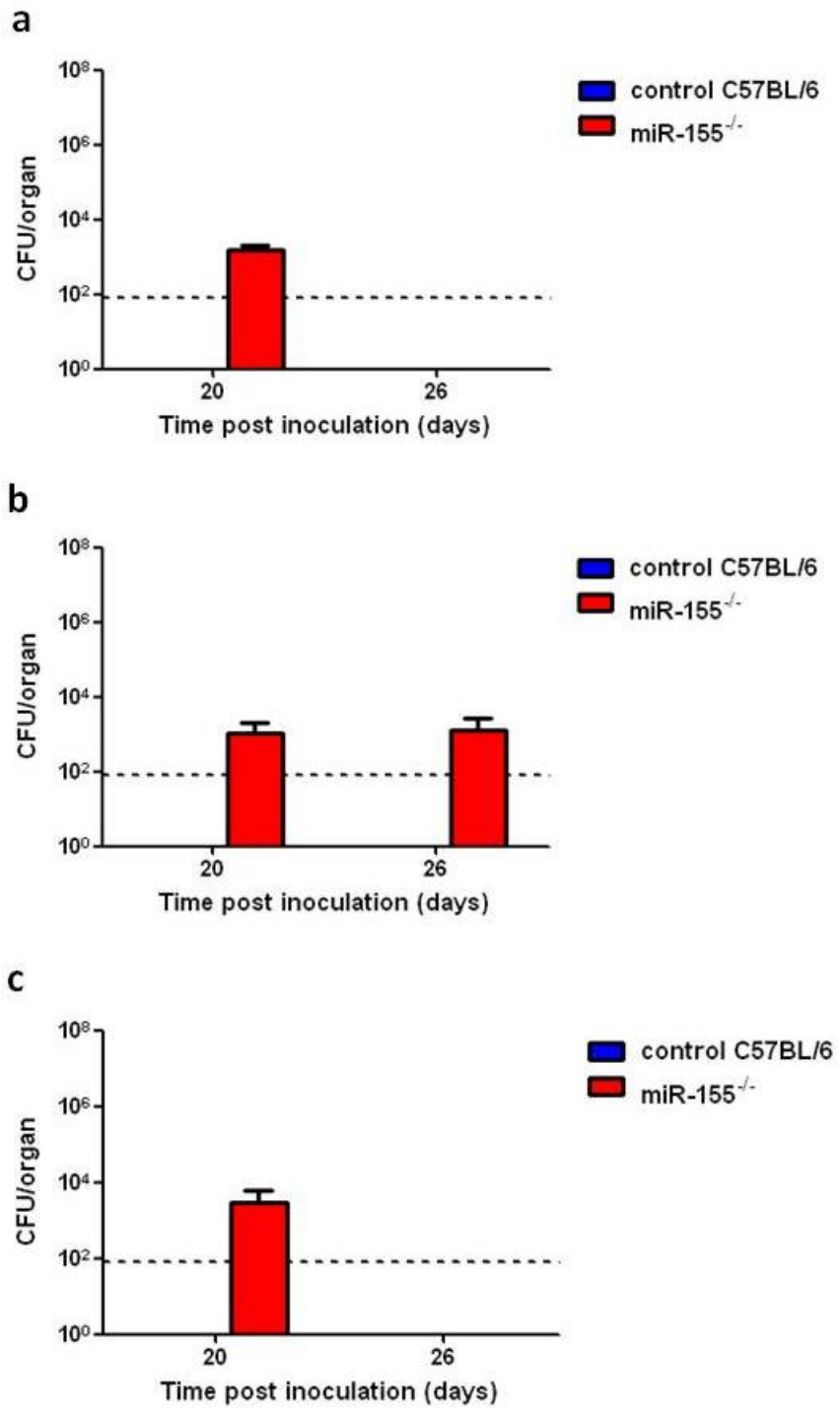

Figure 35. miR-155-deficient mice exhibit systemic spread of *C. rodentium*.

miR-155-deficient (red bars) and control C57BL/6 (blue bars) mice were orally infected with *C. rodentium.* On days 20 and 26 pi, mice were sacrificed and numbers of *C. rodentium* (±SEM) in systemic tissues; mesenteric lymph nodes(a), spleen (b)and liver (c) were enumerated, n=5 mice per group. Broken lines indicate the detection level of the assay.

3.2.7 miR-155-deficient mice mount a blunted humoral immune responses to *C. rodentium*

The previous data suggests that miR-155 is important for the development of full protective immunity to *C. rodentium* as miR-155-deficient mice are hyper-susceptible to infection. However, a more defined role for this microRNA still remained to be elucidated. Given that the phenotype we observed in *C. rodentium* infected miR-155-deficient mice closely resembled that observed in μMT (B-cell deficient) and RAG2-deficient (lacking B and T cells) mice, we speculated that the susceptibility of miR-155-deficient mice might be due to impaired antibody responses. Thus, we assessed serum antibody responses against the *C. rodentium* surface-associated protein EspA in miR-155-deficient and C57BL/6 mice at 14 and 45 days after infection. EspA filaments are essential for mediating A/E lesion formation and are normally targeted by host antibody responses[171]. We found that while infected wild-type mice developed a robust antibody response to *C. rodentium* by day 14 pi, miR-155-deficient mice produced significantly reduced levels of EspA-specific Ig, IgG and IgA (Figure 36a, b and e). Furthermore, when antibody responses were examined 45 days pi, miR-155-deficient mice demonstrated significantly diminished anti-*Citrobacter* serum IgG responses compared to C57BL/6 mice (Figure 36f and g). Recent reports have demonstrated that while the production and transport of secretory antibodies is not detectably required for clearance of *C. rodentium*, non-secretory IgG antibodies are extremely important for passive immune protection[172].

In addition, C57BL/6 mice infected with *C. rodentium* also mounted EspA-specific IgA responses in supernatants of faecal homogenates. Whilst faecal homogenate EspA-specific IgA titres were highly variable in C57BL/6 mice we observed that miR-155-deficient mice had dramatically diminished titres at all time points assayed (Figure 37).

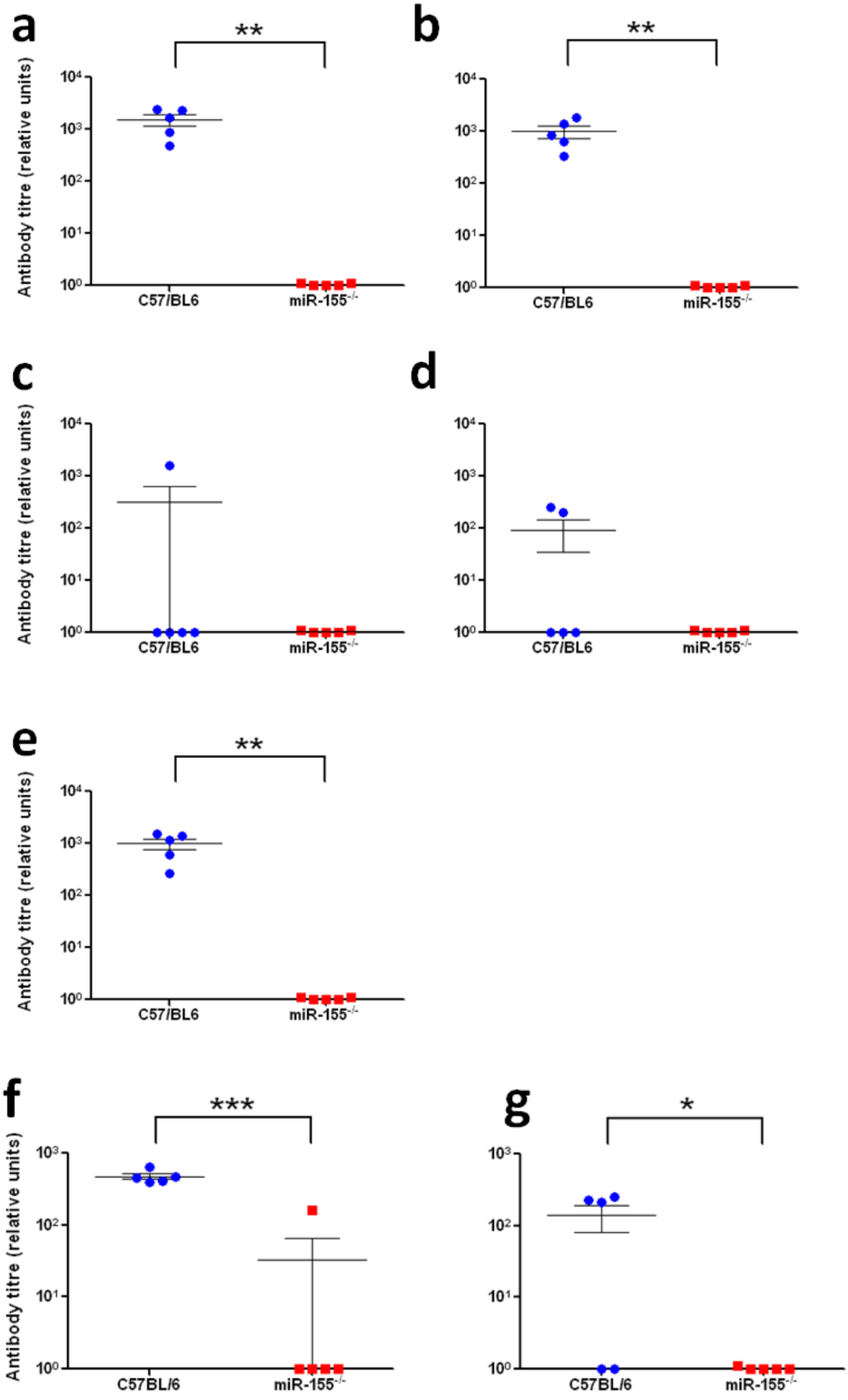
a
b
c
d
e
f
g
Antibody titre (relative units)
C57/BL6
C57BL/6
miR-155-/-
**
***
*

Figure 36. Humoral immune responses to *C. rodentium* surface protein EspA

Serum antibody responses against the *C. rodentium* surface-associated protein EspA in C57BL/6 (blue circles) and miR-155-deficient (red squares) mice at 14 and 45 days pi with *C. rodentium*. Relative titres (± SEM) of anti-EspA serum Ig (a), IgG (b), IgG1 (c), IgG2 (d), and IgA (e) at day 14 pi were calculated. Relative titres of anti-EspA serum Ig (f) and IgG (g) at 45 days after infection. The outlying data point observed in the anti-EspA serum Ig titres of miR-155-deficient mice at 45 days after infection could have arisen either as a result of human or instrument error or could simply be due to natural deviation within the population of mice. As we could not be ascertained that this deviation was not significant we did not exclude this outlier from our analysis.

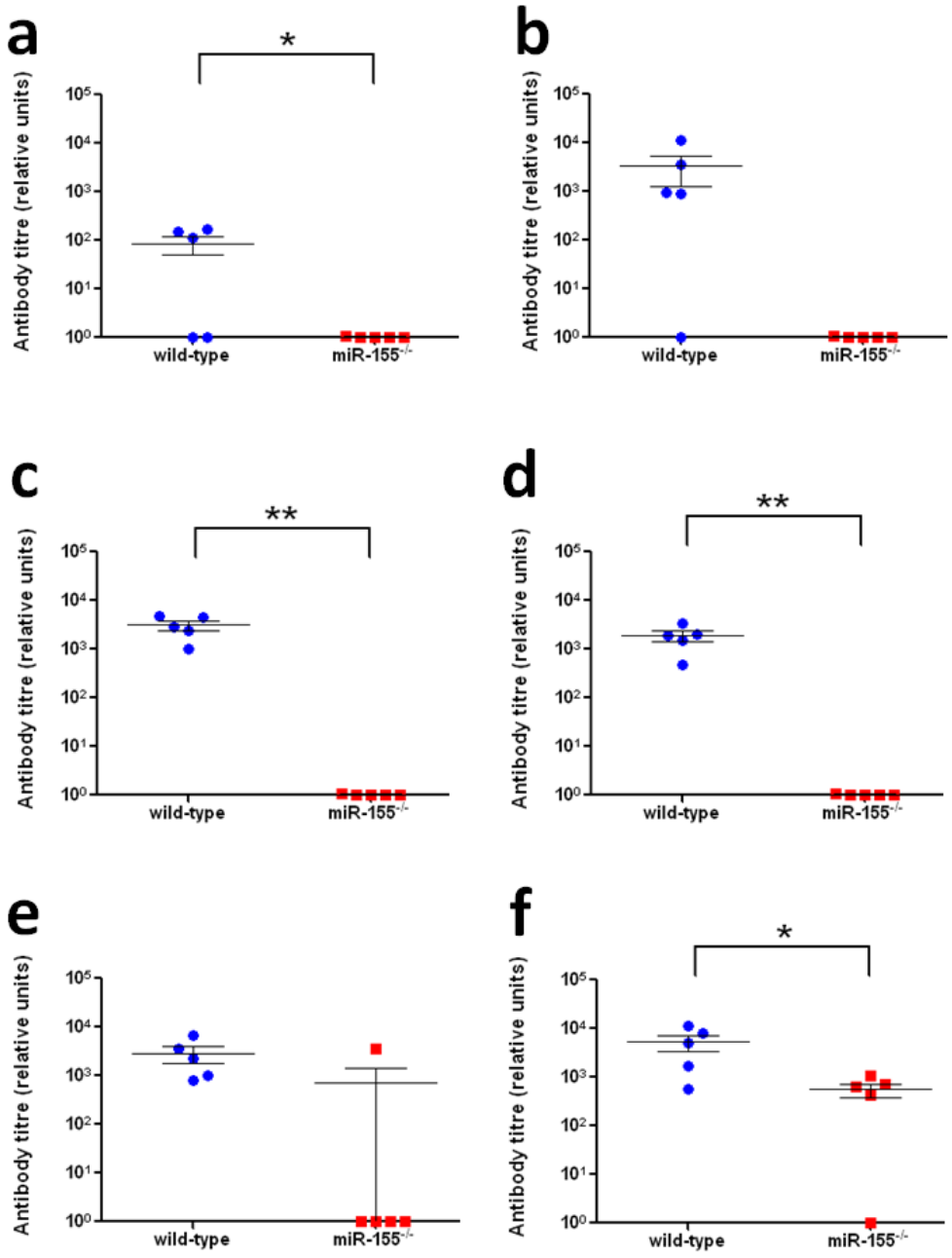

Figure 37. Faecal IgA responses to *C. rodentium* surface protein EspA

Relative titres of faecal IgA (± SEM) responses against the *C. rodentium* surface-associated protein EspA in C57BL/6 (blue circles) and miR-155-deficient (red squares) mice at 8 (a), 11 (b), 14 (c), 18 (d), 21 (e) and 30 (f) days pi with *C. rodentium*. The outlying data point observed in faecal IgA titres from miR-155-deficient mice at 21 days after infection could have arisen either as a result of human or instrument error or could simply be due to natural deviation within the population of mice. As we could not be ascertained that this deviation was not significant we did not exclude this outlier from our analysis.

3.2.8 Germinal centre formation is adversely affected in infected miR-155-deficient mice

Germinal centres develop in the primary B cell follicles of secondary lymphoid organs and support the generation of memory B cells and plasma cells capable of producing high affinity pathogen-specific class-switched antibodies[73, 74, 77, 94, 96, 97, 101, 209]. During infection with *C. rodentium* germinal centres rapidly develop in GALT, especially the mLNs. Previous studies have reported a requirement of miR-155 during regulation of the germinal centre response and generation of class-switched plasma cells[33, 34]. Accordingly, we wanted to study germinal centre formation in the mLNs of miR-155-deficient following infection with *C. rodentium*.

Examination of mLNs from naive miR-155-deficient mice revealed that there were no obvious abnormalities in the development of primary B cell follicles (Figure 38a and b). However, we observed that there were significantly fewer germinal centres in the mLNs of miR-155-deficient mice 14 days after infection compared to control C57BL/6 mice (Figure 38c, d and e). Moreover, the germinal centres formed in miR-155-deficient mice were noticeably smaller in size (Figure 38c, d and f).

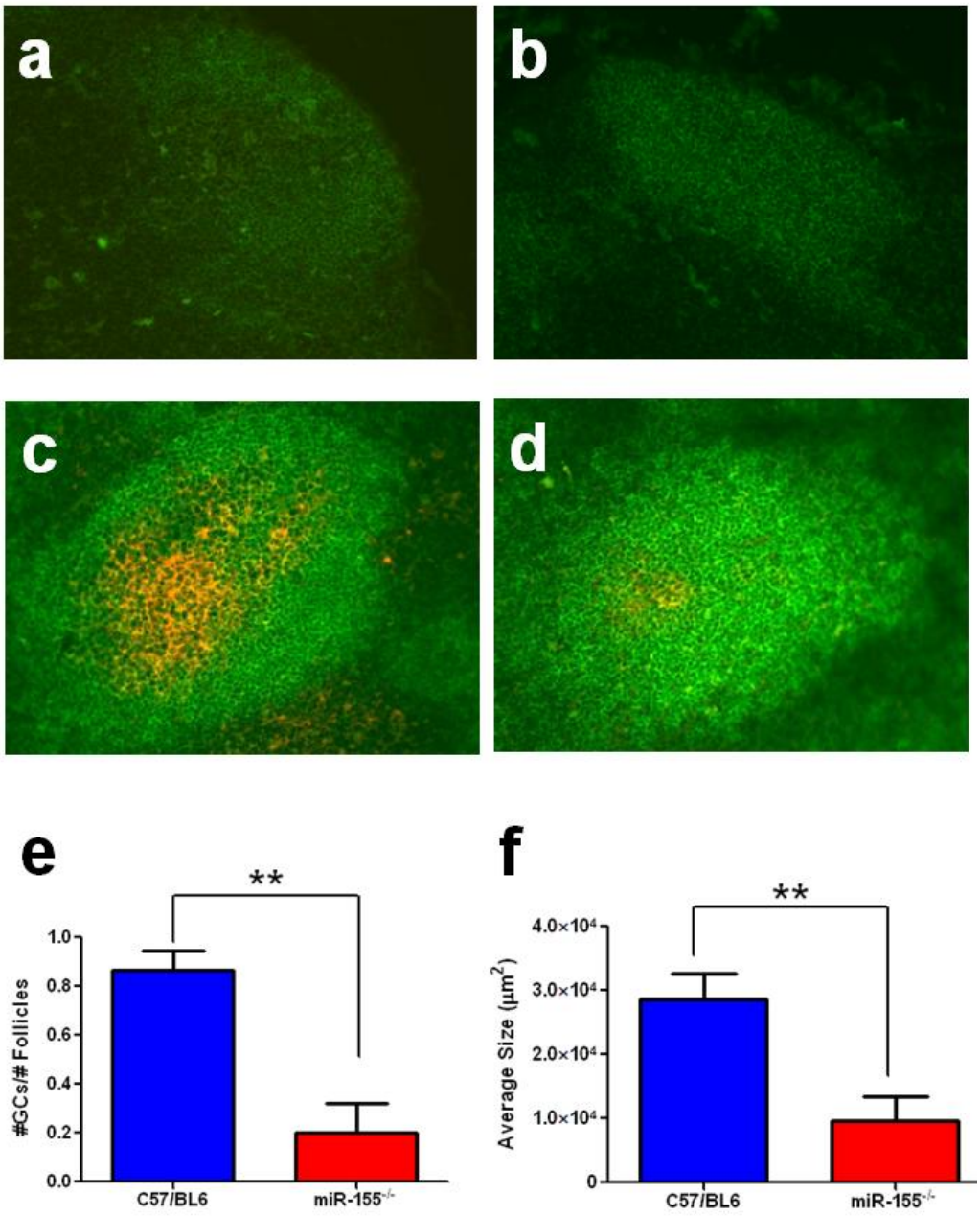

Figure 38. Germinal centre formation in C57BL/6 and miR-155-deficient mice following infection with *C. rodentium*.

C57BL/6 and miR-155-deficient mice were infected orally with *C. rodentium* and germinal centre formation was analyzed 14 days pi. Immunohistochemistry was performed on mLNs from naive C57BL/6 (a), naive miR-155-deficient (b), infected C57BL/6 (c) and infected miR-155-deficient (d) mice 14 days pi to detect germinal centres, magnification x40 (Green, $B220^{+}$; Red/Orange, PNA^{+}). Number (e) and size (f) of GCs (±SEM) was determined from sections; n = 4 mice per group.

Additionally, we wanted to look at germinal centre formation in the caecal patch, a specialised lymphoid tissue in the caecum and initial site of colonisation during *C. rodentium* infection. However, due to technical difficulties we were unable to use conventional immunofluorescent staining to follow the development of germinal centres. Upon analysis of toluidine blue – stained caecal patch sections from C57BL/6 and miR-155-deficient mice 14 days after infection, we observed that the latter contained markedly fewer tingible body macrophages (TBMs), a characteristic feature of germinal centres (Figure 39). TBMs are unique, large [20 to 30 microns (μ)] phagocytic cells that reside in close proximity to antigen-retaining FDCs in germinal centres of secondary lymphoid organs. These cells were first identified because they appeared in lymphoid organs following antigenic stimulation and contained many phagocytised, chromatin-condensed apoptotic cells (called tingible bodies) in varying stages of lysis. Recent studies have shown that centrocytes that have undergone somatic hypermutation leading to the expression of low affinity antigen receptors do not receive essential survival signals and are thus condemned to apoptose. The apoptotic centrocytes are rapidly and efficiently removed by TBMs[102, 210]. We tentatively speculate that the decreased numbers of TBMs observed in caecal patch sections from miR-155-deficient mice may indicate that germinal centre formation is diminished not only in mLNs but also in the lymphoid tissue of the caecum. But perhaps most importantly the lack of TBMs in miR-155-deficient mice indicates that there may not be as high a death rate among miR-155-deficient plasmablasts as has been suggested previously[34]. Consequently, it is possible that the lack of miR-155 prevents the majority of B cells from differentiating into plasmablasts.

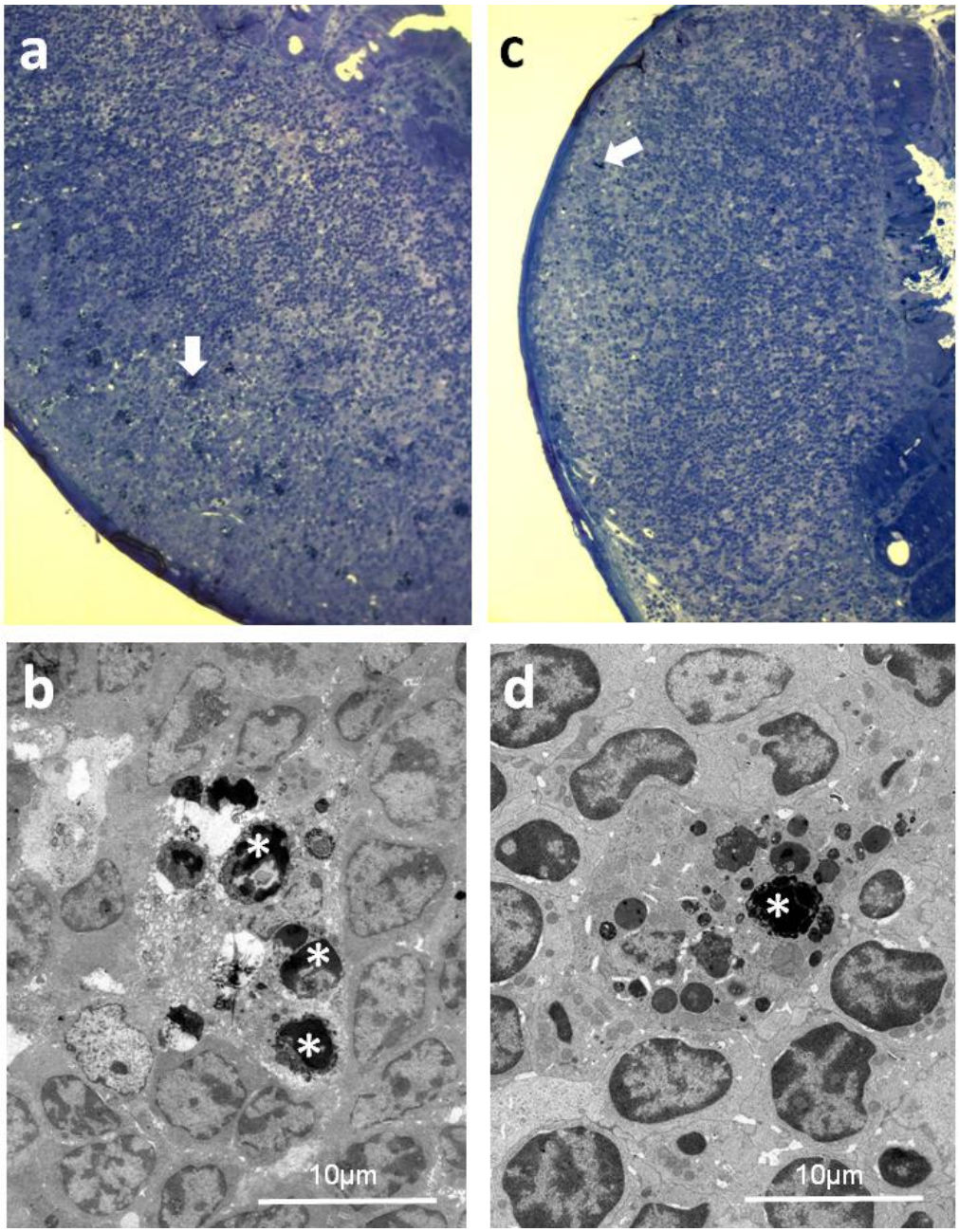

Figure 39. Presence of tingible body macrophages in the caecal patches of C57BL/6 and miR-155-deficient mice 14 days after infection with *C. rodentium*

Toluidine blue staining and transmission electron microscopy of caecal patch sections from infected C57BL/6 and miR-155-deficient mice, 14 days pi. Sections stained with toluidine blue demonstrate that there is an abundance of TBMs (arrow) in control C57BL/6 mice (a), whereas miR-155-deficient mice contain considerably fewer TBMs (c), magnification x20. A transmission electron micrograph showing of a tingible body macrophage from germinal centre of C57BL/6 (b) and miR-155-deficient (d) mice, containing a variable number of tingible bodies (asterisk) in varying stages of degradation.

3.2.9 Genome-wide analysis of gene expression in *C. rodentium* infected tissues

The primary mode of action of miR-155 is through specific mRNA targeting. In view of the fact that animal miRNAs have been shown to regulate large numbers of target mRNAs and the finding that miR-155 is expressed in numerous different cell types following activation, we conducted microarray analysis on infected tissues from C57BL/6 and miR-155-deficient mice, with the aim identifying key components of the immune system which dysfunction in the absence of miR-155, *in vivo*.

Mice were orally infected with *C. rodentium* and total RNA was extracted from the caecal patch and colon at 4 and 14 days pi. Gene expression levels in miR-155-deficient mice were then related to a parallel cohort of infected control C57BL/6 mice. We initially chose to examine the gene expression profiles in these specific tissues, at these particular time points for two reasons. Firstly, we know from previous studies looking at the colonisation dynamics of *C. rodentium* that, the caecal patch and colon are the main sites of infection[161]. Primary colonization of the mouse by *C. rodentium* occurs within the caecal patch, just hours after receiving 10^9 organisms of *C. rodentium* orally. Within 2-4 days, the infection becomes established in the distal colon. In C57BL/6 mice the peak of infection in the colon occurs at around days 5-14, and is accompanied by colonic crypt hyperplasia. Normal immunocompetent mice are capable of mounting a protective sterilising immune response and consequently completely clear infection by day 21 pi. Secondly, from our research we find that from 4-14 days pi the numbers of *C. rodentium* within the caecal patch and colon of miR-155-deficient mice are comparable with control C57BL/6 mice. However, after day 14 pi whilst control mice begin clearing infection, miR-155-deficient mice remain heavily infected in addition to developing grossly exaggerated colonic hyperplasia.

To gain an even greater insight into how the absence of miR-155 affects global gene-expression, gene expression data was further analysed using Innate DB (www.innatedb.ca), a comprehensive database and analysis

platform that enables testing for over-representation of differentially expressed genes in greater than 2,500 known innate immune response pathways, sourced from several of the publicly available pathway databases[211]. Additionally, it provides us with a useful tool for conducting comprehensive network analysis, for the identification of signalling cascades and functionally relevant sub-networks involving molecular interactions between differentially expressed genes and their non-differentially expressed interacting partners. Using network analysis it is possible to identify key regulators of gene expression, which exert their effects through protein modification or other non-transcriptional mechanisms.

Differentially expressed mRNAs were only considered significant if they were altered by at least 1.5 fold and had an adjusted P-value of less than 0.05. Using these strict criteria, we found that 314 genes (229 up- and 85 down-regulated) on day 4 and 8 genes (7 up- and 1 down-regulated) on day 14 pi were differentially expressed in miR-155-deficient caecal patches, compared with infected controls (Table S1-4 and S10-13). Perhaps surprisingly, in colon samples taken from infected miR-155-deficient mice we found that only 3 genes (1 up-and 2 down-regulated) on day 4 pi and 7 genes (7 up-regulated) on day 14 pi were reproducibly significantly differentially expressed, far less than might be expected given the gross changes in pathology, increased pathogen burden and prolonged clearance time (Table S19-22 and S28-31). This lack of reproducible differential regulation in the colon could be due in part to the significant pathological changes occurring in these tissues, perhaps causing significant variations in cell populations.

However, whilst transcriptional profiling allows the analysis of a large number of genes simultaneously, due to the statistical issue of multiple testing it can be susceptible to producing false-positive results. To overcome this problem we selected 6 genes of interest that were differentially expressed in miR-155-deficient mice and reanalyzed them using Real-Time PCR (or reverse transcriptase real-time PCR) with SYBR green. Real-Time PCR (RT-PCR) was performed on cDNA synthesized from the same total RNA used as templates for the cDNA probes hybridised to the arrays. All genes tested

changed in the same direction as they had on the arrays thus, the RT-PCR results agreed well with the microarray results (Figure 40c and d).

3.2.9.1 Transcriptional profiling of *C. rodentium*-infected ceacal patches reveals that B cell function is affected in the absence of miR-155, on day 4 pi

Global gene expression analysis revealed that 314 genes were significantly differentially expressed in the caecal patch of miR-155-deficient mice, 4 days after *C. rodentium* infection. A total of 229 genes were up-regulated while 85 genes were decreased in expression. Because we were concerned with genes that are important for host defence during *C. rodentium* infection, we focused primarily on genes that have an immunomodulatory role. Of the 85 genes down-regulated in miR-155-deficient caecal patches on day 4 pi, we observed that a considerable number, approximately 17 percent, have a reported immune function. Furthermore, we noted that many of the genes are involved, at some stage, in the differentiation and/or function of B cells (Figure 40a). For example CD19 has a role in germinal center formation, B cell homing and apoptosis. Similar to miR-155-deficient mice, CD19 null mice have decreased mitogenic responses, low germinal center formation and decreased humoral immune responses to T cell-independent type 1- and T cell-dependent antigens. In addition, Bcl6 is essential for the differentiation of germinal center B cells since Bcl6 null mice have severely impaired germinal center formation. When we further analysed the expression data using KEGG pathway analysis, and the data analysis and pathway over-representation analysis tools in InnateDB, the B cell receptor (BCR) signalling pathway was identified as being significantly associated with down-regulated genes (Table S6, S8 and S9 and Figure S1). These data together with our results thus far suggest that BCR signalling and consequently B cell function is adversely affected in miR-155-deficient mice. This finding is consistent with previously published reports which have shown that miR-155 is expressed upon BCR cross-linking and CD40 stimulation[23, 34].

It is also worth noting that the most significantly down-regulated gene in the caecal patch on day 4 pi was matrix metalloproteinase-3 (or stomelysin-1) (Table S3 and S4). Matrix metalloproteinase-3 (MMP3) is a member of the matrix metalloproteinase family, a group of molecules which are involved in mediating matrix remodelling and cell migration during tissue injury and repair. A recent study has found that MMPs are strongly induced in epithelial cells during bacterial infections. MMP3, in particular, was shown to be extremely important during infection with *C. rodentium*[212]. MMP3-deficient mice infected with *C. rodentium* exhibited delayed clearance of bacteria from the colon as a result of delayed migration of $CD4^+$ T lymphocytes into the intestinal lamina propria and reduced transcription of TNF-α. MMP3 is thought to function by opening up tight junctions between endothelial cells subsequently enabling lymphocytes to migrate through. In support of this hypothesis, it has been shown that treatment of mice with MMP inhibitors results in an accumulation of lymphocytes on the lymph node endothelium and reduced diapedesis. Accordingly, KEGG testing for overrepresentation amongst the down-regulated genes showed that there was an overrepresentation of genes involved in leukocyte transendothelial migration (Table S6). Thus, it is possible that lymphocyte migration may be affected in miR-155-deficient mice and analysis of their movements during infection will be an important topic for future studies.

Lastly, we sought to identify whether differentially expressed mRNAs represent direct miR-155 targets. To this end, we analysed the 3'UTRs of mRNAs for the presence of miR-155 seed matches using a target prediction algorithm, called Sylamer[213]. We found that there was no significant enrichment or depletion of miR-155 seed sequences amongst the differentially expressed genes (Figure S2). There are two possible explanations for this, firstly the differentially expressed genes may represent indirect miR-155 targets or alternatively, secondary effects such as differential recruitment and activation of cells may be occurring above the direct effects of miR-155.

a

Target Identification	Symbol	Fold Change	Adjusted P-Value	GO Biological Process
scl37307.8.1_29-S	Mmp3	-3.79	0.00669	peptidoglycan metabolic process (GO:0000270) | proteolysis (GO:0006508) | collagen catabolic process (GO:0030574)
scl48501.9_645-S	Cd86	-1.68	0.0127	defense response (GO:0006952)
scl38155.8_378-S	Tnfaip3	-1.99	0.0136	ubiquitin cycle (GO:0006512) | apoptosis (GO:0006915)
scl25940.13_350-S	Lat2	-1.92	0.0144	immune response (GO:0006955) | B cell activation (GO:0042113) | mast cell degranulation (GO:0043303) | B cell receptor signaling pathway (GO:0050853)
scl0003597.1_94-S	Mmp3	-2.45	0.0152	peptidoglycan metabolic process (GO:0000270) | proteolysis (GO:0006508) | collagen catabolic process (GO:0030574)
scl37305.10.1_6-S	Mmp10	-2.02	0.0187	peptidoglycan metabolic process (GO:0000270) | proteolysis (GO:0006508) | collagen catabolic process (GO:0030574)
scl48625.8_280-S	Bcl6	-1.93	0.0341	negative regulation of transcription from R- polymerase II promoter (GO:0000122) | cell morphogenesis (GO:0000902) | negative regulation of cell-matrix adhesion (GO:0001953) | germinal center formation (GO:0002467) | negative regulation of T-helper 2 type immune response (GO:0002829) | transcription (GO:0006350) | regulation of transcription, D--dependent (GO:0006355) | Rho protein signal transduction (GO:0007266) | spermatogenesis (GO:0007283) | protein localization (GO:0008104) | negative regulation of cell proliferation (GO:0008285) | actin cytoskeleton organization and biogenesis (GO:0030036) | B cell differentiation (GO:0030183) | positive regulation of B cell proliferation (GO:0030890) | regulation of Rho GTPase activity (GO:0032319) | negative regulation of mast cell cytokine production (GO:0032764) | negative regulation of Rho protein signal transduction (GO:0035024) | T-helper 2 type immune response (GO:0042092) | regulation of cell proliferation (GO:0042127) | negative regulation of apoptosis (GO:0043066) | regulation of memory T cell differentiation (GO:0043380) | negative regulation of cell differentiation (GO:0045596) | negative regulation of T-helper 2 cell differentiation (GO:0045629) | negative regulation of isotype switching to IgE isotypes (GO:0048294) | erythrocyte development (GO:0048821) | regulation of inflammatory response (GO:0050727) | positive regulation of cell motility (GO:0051272)
scl30689.14.1_1-S	Cd19	-1.98	0.0377	-
scl0012514.2_91-S	Cd68	-1.56	0.038	-
scl41469.8_427-S	Tnfrsf13b	-2.18	0.0401	B cell homeostasis (GO:0001782) | immune response (GO:0006955) | negative regulation of B cell proliferation (GO:0030889)
scl38756.3.1_44-S	Vpreb3	-2.27	0.0404	-
scl21758.4.1_5-S	Cd2	-1.67	0.0404	protein amino acid phosphorylation (GO:0006468) | defense response (GO:0006952) | cell adhesion (GO:0007155)
scl44840.4_185-S	Cd83	-2.26	0.0449	-
scl44948.10_526-S	Irf4	-1.6	0.0458	transcription (GO:0006350) | regulation of transcription, D--dependent (GO:0006355) | myeloid dendritic cell differentiation (GO:0043011)

b

Target Identification	Symbol	Fold Change	Adjusted P-Value	GO Biological Process
scl53984.2_610-S	Cxcr3	-1.52	0.0361	chemotaxis (GO:0006935) | defense response (GO:0006952) | signal transduction (GO:0007165) | G-protein coupled receptor protein signaling pathway (GO:0007186)

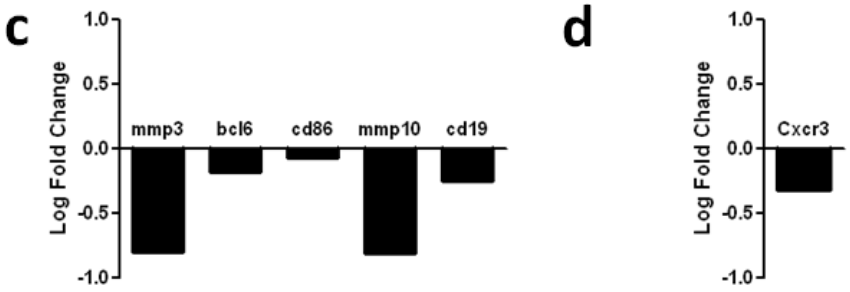

Figure 40. Genome-wide analysis of gene expression in *C. rodentium* infected tissues

Gene expression profiling in *C. rodentium*-infected tissues. miR-155-deficient and control C57BL/6 mice were infected orally with *C. rodentium* and transcriptional responses in infected caecal patches and colon sections were analysed 4 and 14 days pi. Immunomodulatory genes and genes involved in B cell differentiation and/or function (grey) that were significantly down-regulated in miR-155-deficient caecal patches on days 4 (a) and 14 (b) after infection, compared with control mice. We selected six genes of interest that were differentially expressed in miR-155-deficient mice and reanalyzed them using RT-PCR, all genes tested changed in the same direction as they had on the arrays (c and d).

3.2.9.2 Loss of miR-155 results in the up-regulation of genes involved in metabolism, catabolism and biosynthesis

Analysis of genes up-regulated in miR-155-deficient caecal patches 4 days after infection showed that there was no enrichment for genes involved in the immune response. However perhaps interestingly, Gene Ontology (GO) and KEGG Pathway analysis revealed that there was an over-representation of genes involved in a number of different metabolic, biosynthetic and catabolic processes as well as ion transport (Table 13, S5 and S7).

The intestine is a complex ecosystem involving the interactions of a diverse microbial community with the physiology, genetics and behaviour of the animal host. Bacterial colonisation in the intestine is essential for many normal physiological processes, such as enhancing intestinal development and contributing to the host's nutrition but also for immune system development and defence against pathogens. The microbiota is known to play an essential role in 'colonization resistance' whereby resident commensal bacteria prevent the growth of many pathogenic bacteria by competing with them for space, nutrients and host-receptors in addition to producing metabolic bi-products with anti-microbial properties. We are only just beginning to understand the complex, mutually beneficial, symbiotic relationship that exists between the host and the intestinal microbiota but prior experiments have shown that certain nutritional factors can modify the composition of flora residing in the gut. Bärbel Stecher and Wolf-Dietrich Hardt have recently reviewed 'The food hypothesis' which speculates that increased nutrient availability and fewer inhibitory substances in the gut provide ideal conditions for growth of pathogenic organisms[38]. They suggest that in the normal gut, high energy nutrients are scarce and any available nutrients are used up efficiently by the microbiota. Consequently, the severe nutrient limitations inhibit the growth of incoming pathogens. However, whilst steady growth conditions and a limited nutrient supply help to stabilize the resident microbiota population structure, considerable shifts in nutrient range and availability (such as those seen

during infection and inflammation) allow the outgrowth of bacterial species that grow at high rates on these substrates. For example, enteropathogens such as *Salmonella* spp., pathogenic *E. coli* spp., *Shigella* spp., *Citrobacter* spp., and *Vibrio cholerae* exhibit rapid growth on nutrient rich media, in the laboratory. In 1977, Barthold *et al* suggested a role for gut flora in transmissible murine colonic hyperplasia (TMCH) after it was found that the severity of hyperplasia during infection with *C. rodentium* could be modified not only by host strain and species but also by the diets fed to inoculated mice. It is thus possible that the up-regulation of metabolism, catabolism, biosynthesis and ion transport in miR-155-deficient mice might perturb the composition of intestinal flora and contribute to the increased severity of infection. However, the relative availability of nutrients in the infected gut and their subsequent utilisation by *C. rodentium* and commensal microbiota has yet to be analyzed quantitatively.

GOBPID	Pvalue	OddsRatio	ExpCount	Count	Size	Term
GO:0006631	9.7e-07	5.3	3.30	15	133	fatty acid metabolic process
GO:0019752	3.8e-05	2.9	8.45	22	342	carboxylic acid metabolic process
GO:0044255	6.1e-05	3.2	6.31	18	270	cellular lipid metabolic process
GO:0006816	2.5e-04	4.8	2.11	9	85	calcium ion transport
GO:0006812	3.1e-04	2.5	9.10	21	367	cation transport
GO:0050801	5.9e-04	3.3	3.94	12	159	ion homeostasis
GO:0055082	1.2e-03	3.2	3.70	11	149	cellular chemical homeostasis
GO:0008272	1.6e-03	17.0	0.25	3	10	sulfate transport
GO:0001523	2.1e-03	14.9	0.27	3	11	retinoid metabolic process
GO:0006694	2.5e-03	4.8	1.38	6	56	steroid biosynthetic process
GO:0030003	3.6e-03	3.8	1.98	7	80	cellular cation homeostasis
GO:0042445	4.2e-03	4.3	1.54	6	62	hormone metabolic process
GO:0006766	7.1e-03	4.5	1.22	5	49	vitamin metabolic process
GO:0051234	8.9e-03	1.4	47.55	63	1917	establishment of localization
GO:0006829	1.3e-02	7.0	0.50	3	20	zinc ion transport
GO:0042493	1.3e-02	7.0	0.50	3	20	response to drug
GO:0055066	1.3e-02	3.3	1.93	6	78	di-, tri-valent inorganic cation homeostasis
GO:0030155	1.3e-02	4.8	0.92	4	37	regulation of cell adhesion
GO:0006732	1.7e-02	2.8	2.65	7	107	coenzyme metabolic process
GO:0006639	1.9e-02	6.0	0.57	3	23	acylglycerol metabolic process
GO:0006814	1.9e-02	3.0	2.11	6	85	sodium ion transport
GO:0008366	2.1e-02	5.7	0.60	3	24	axon ensheathment
GO:0008015	2.1e-02	3.0	2.16	6	87	blood circulation
GO:0006790	2.3e-02	4.0	1.09	4	44	sulfur metabolic process
GO:0006941	2.3e-02	5.4	0.62	3	25	striated muscle contraction
GO:0019228	2.3e-02	5.4	0.62	3	25	regulation of action potential in neuron
GO:0006721	2.4e-02	9.9	0.25	2	10	terpenoid metabolic process
GO:0007431	2.4e-02	9.9	0.25	2	10	salivary gland development
GO:0030865	2.4e-02	9.9	0.25	2	10	cortical cytoskeleton organization and biogenesis
GO:0006811	2.6e-02	2.2	4.22	9	179	ion transport
GO:0042592	3.1e-02	1.8	8.04	14	324	homeostatic process
GO:0002009	3.3e-02	2.6	2.41	6	97	morphogenesis of an epithelium
GO:0002026	3.4e-02	7.9	0.30	2	12	regulation of the force of heart contraction
GO:0009069	3.4e-02	7.9	0.30	2	12	serine family amino acid metabolic process
GO:0042364	3.4e-02	7.9	0.30	2	12	water-soluble vitamin biosynthetic process
GO:0006081	4.0e-02	7.2	0.32	2	13	aldehyde metabolic process
GO:0008152	4.1e-02	1.3	133.96	148	5400	metabolic process
GO:0001501	4.3e-02	2.1	3.92	8	158	skeletal development
GO:0044242	4.3e-02	4.1	0.79	3	32	cellular lipid catabolic process
GO:0006776	4.6e-02	6.6	0.35	2	14	vitamin A metabolic process
GO:0007339	4.6e-02	6.6	0.35	2	14	binding of sperm to zona pellucida
GO:0043506	4.6e-02	6.6	0.35	2	14	regulation of JNK activity

Table 13. GO conditional test for over-representation of genes up-regulated in miR-155-deficient caecal patches, 4 days after infection.

3.2.9.3 Chemokine (C-X-C motif) receptor 3 (CXCR3) is down-regulated in miR-155-deficient caecal patches 14 days after infection with *C. rodentium*

On day 14 pi, there appeared to be little detectable transcriptional difference between the caecal patches from miR-155-deficient mice and those from controls (Table S10, S11, S12 and S13). In fact, CXCR3 was the only gene identified as being significantly down-regulated at this time point (Figure 40b and Table S12 and S13). CXC chemokines are rapidly induced in the colons of mice infected with *C. rodentium,* and are critical chemoattractants and activators of leukocyte subsets[214]. CXCR3 is one of a number of CXC chemokine receptors which bind CXC chemokines. A recently published report has shown that CXCR3 and its cognate ligands have a physiological function in mucosal defence against *C. rodentium*[214]. *C. rodentium*-infected CXCR3-deficient mice display significantly increased faecal CFU at 14 and 17 days after infection as well as higher pathogen burdens in the liver and spleen. Analysis of antibody titres against *C. rodentium* showed that deficiency of CXCR3 results in significantly delayed induction of specific IgG responses, but not IgM[214]. CXCR3 is predominantly expressed on activated T cells, particularly T_h1 cells[214]. As discussed previously, T_h1 cells are extremely important for the clearance of a *C. rodentium* infection because they produce large amounts of IFN-γ which stimulates the bacterial killing capacity of phagocytic cells and they additionally provide essential help to B cells for the generation of specific IgG responses[167-171]. In mice, IFN-γ induces the expression of CXCR3 on memory B cells and plasma cell precursors, which is likely to further aid in the generation of *C. rodentium* specific antibody.

Given these data it is possible that the decreased expression of CXCR3 observed in miR-155-deficient mice could affect leukocyte migration and/or activation. In support of this, GO conditional testing for overrepresentation amongst the genes down-regulated in miR-155-deficient caecal patches on day 14 pi, showed that there was a significant overrepresentation of genes

involved in chemotaxis, locomotory behaviour and leukocyte migration (Table S17). In addition, the positive regulation of adaptive immune response based on somatic recombination of immune receptors built from immunoglobulin superfamily domains pathway was also significantly associated with down-regulated genes (Figure S17). This is consistent with previous results suggesting that germinal centre formation and antibody responses are impaired in miR-155-deficient mice following infection with *C. rodentium*.

3.2.9.4 Global gene expression analysis of the colonic response to *C. rodentium* in miR-155-deficient mice reveals only minor differences, despite gross pathological changes

We observed that very few genes were significantly reproducibly differentially expressed in the colons of miR-155-deficient on either day 4 or day 14 after infection (Table S19-22 and S28-31). This was perhaps unexpected given that miR-155-deficient mice develop more severe pathology as well as increased pathogen burdens in the colon after infection (Figure 31, 32 and 33). There are several possible explanations for this; first, unlike the caecal patch which has a significant percentage of B and T cells, the colon consists of more complex populations of cells which change rapidly during the course of infection. Given the considerable changes in cell populations that take place in infected animals it is possible that the background noise in these samples may have masked any underlying trends within specific cells. Secondly, this type of analysis can only identify miRNA targets that have altered mRNA levels. In animals, because there is only partial miRNA pairing to target mRNAs, regulation is thought to act mainly through translational repression rather than mRNA cleavage. Thus it is possible that by using this method we may miss some miR-155 targets that are regulated at the protein level.

Despite the apparent lack of significantly differentially expressed genes, we analysed all the differentially expressed (up- and down-regulated) genes using the analysis tools in InnateDB, GO and KEGG. As observed in the caecal patch samples, GO conditional testing showed that there was a significant overrepresentation of genes involved in numerous different metabolic, catabolic and biosynthesis pathways amongst the up- and down-regulated genes in miR-155-deficient colons, 4 days after infection (Table S25 and S26). In addition, while the immune response-activating cell surface receptor signalling pathway and I-κβ Kinase/NF-κβ cascade were found to be

significantly associated with down-regulated genes, a number of immune response pathways were conversely associated with up-regulated genes, these included the inflammatory response, acute-phase response, leukocyte migration and phosphoinositide-mediated signalling pathways (Table S25 and S26).

On day 14 after infection, we found that an overwhelming number of diverse immune response pathways ranging from leukocyte migration, chemotaxis and activation to antigen processing and presentation were significantly overrepresented amongst the down-regulated genes, according to GO conditional analysis (Table S35). This finding was further supported by InnateDB analysis which additionally identified several immune response pathways highly associated with down-regulated genes (Table S36). These included, the IL-7 signalling (JAK1 JAK3 STAT5) pathway, phosphorylation of CD3 and TCR zeta chains pathway, T cell receptor signalling pathway as well as CD4 T cell receptor signalling (through Vav, Rac and JNK cascade) pathway, immunoregulatory interactions between a Lymphoid and a non-Lymphoid cell pathway, Natural killer (NK) cell mediated cytotoxicity pathway and Translocation of ZAP-70 to Immunological synapse pathway (Table S36). Both these analyses highlight the global disruption caused by the loss of miR-155; it suggests that multiple different cell types and signalling pathways may be affected in colons of miR-155-deficient mice. However, many of the pathways identified as being greatly associated with differentially expressed genes were not significant after correction for multiple testing and thus should be interpreted with extreme caution.

3.3 Phenotype is recapitulated in miR-155-deficient, µMT-deficient chimeric mice

Our data strongly suggests that BCR signalling and B cell function is overwhelmingly disrupted in miR-155-deficient mice, we therefore wished to ascertain whether the defect was intrinsic to B cells. Accordingly we created mixed chimeras by transferring 20% of either wild-type or miR-155-deficient bone-marrow cells with 80% of µMT-deficient bone-marrow cells into sub-lethally irradiated µMT mice, as previously described[34]. Since µMT have a deletion of the Ig H chain that halts B cell development (although adult µMT-deficient mice may possess IgA^+ B cells in systemic and mucosal compartments), animals receiving miR-155-deficient bone-marrow will have only miR-155-deficient B cells whilst animals receiving wild-type bone-marrow will have wild-type B cells. The 20/80 ratio favours reconstitution of all other hematopoietic lineages from wild-type precursors. Both groups of chimeras had similar proportions and numbers of B, $CD4^+$, and $CD8^+$ T cells, data not shown.

3.3.1 miR-155-deficient, µMT-deficient chimeras take significantly longer to resolve infection with *C. rodentium*

miR-155-deficient, µMT-deficient and control wild-type, µMT-deficient mice were orally infected with *C. rodentium*. During infection, there were no obvious disease related mortalities amongst either group of chimeric mice. Similar to that observed in miR-155-deficient germ line mice, all miR-155-deficient, µMT-deficient chimeras successfully eradicated infection but remained chronically infected for an additional 11 days, compared with controls, P value < 0.01 (Figure 41).

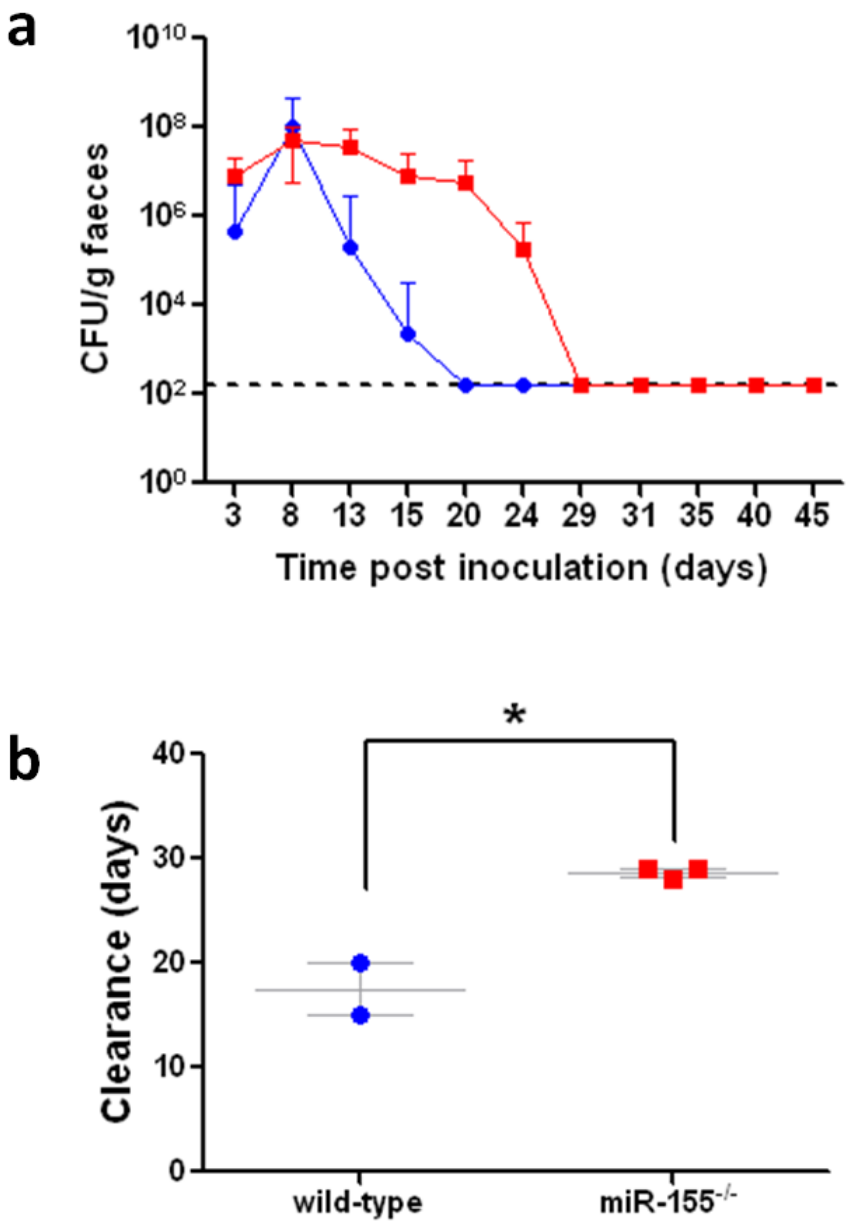

Figure 41. Colonisation and clearance of *C. rodentium* in miR-155-deficient, µMT-deficient and wild-type, µMT-deficient chimeric mice

Susceptibility to *C. rodentium* infection in miR-155-deficient, µMT-deficient chimeric mice. miR-155-deficient, µMT-deficient (Red squares) and wild-type, µMT-deficient (Blue circles) chimeric mice were orally gavaged with approximately $1x10^9$ CFU of *C. rodentium*. (a) Viable *C. rodentium* were enumerated from faecal samples by plating on LB agar supplemented with naladixic acid, n=2 wild-type, µMT-deficient and n=3 miR-155-deficient,

μMT-deficient mice. (b) Time (days) taken to resolve infection (± SEM), * indicates P value <0.01 by Student's t-test.

3.3.2 miR-155-deficient, μMT-deficient chimeras are highly susceptible to *C. rodentium* infection

In an independent experiment, gastrointestinal and systemic tissues were collected from infected mice at various time points pi, and the size of pathogen burden was determined by viable count. On day 14 pi, the pathogen burden in gastrointestinal tissues of miR-155-deficient, μMT-deficient mice were not significantly different than those observed in wild-type, μMT-deficient chimeras (Figure 42). Although unusually, we did observe considerably greater bacterial counts in the colons of wild-type, μMT-deficient chimeras at this time point. Despite there being merely negligible differences between the gastrointestinal burdens of miR-155-deficient, μMT-deficient and wild-type, μMT-deficient mice 14 days after infection, we observed that several miR-155-deficient, μMT-deficient chimeras had a considerably greater burden of *C. rodentium* in liver, spleen and mLN cultures (Figure 43). Thus, providing evidence that miR-155-deficient, μMT-deficient chimeras are less capable in their ability to control a primary mucosal infection and consequently this has lead to systemic spread of *C. rodentium*.

Whilst all wild-type, μMT-deficient chimeras had cleared infection by day 21 after infection, miR-155-deficient, μMT-deficient chimeras remained heavily infected and demonstrated a sizeable burden of *C. rodentium* in the colon, caecum and caecal contents (Figure 42).

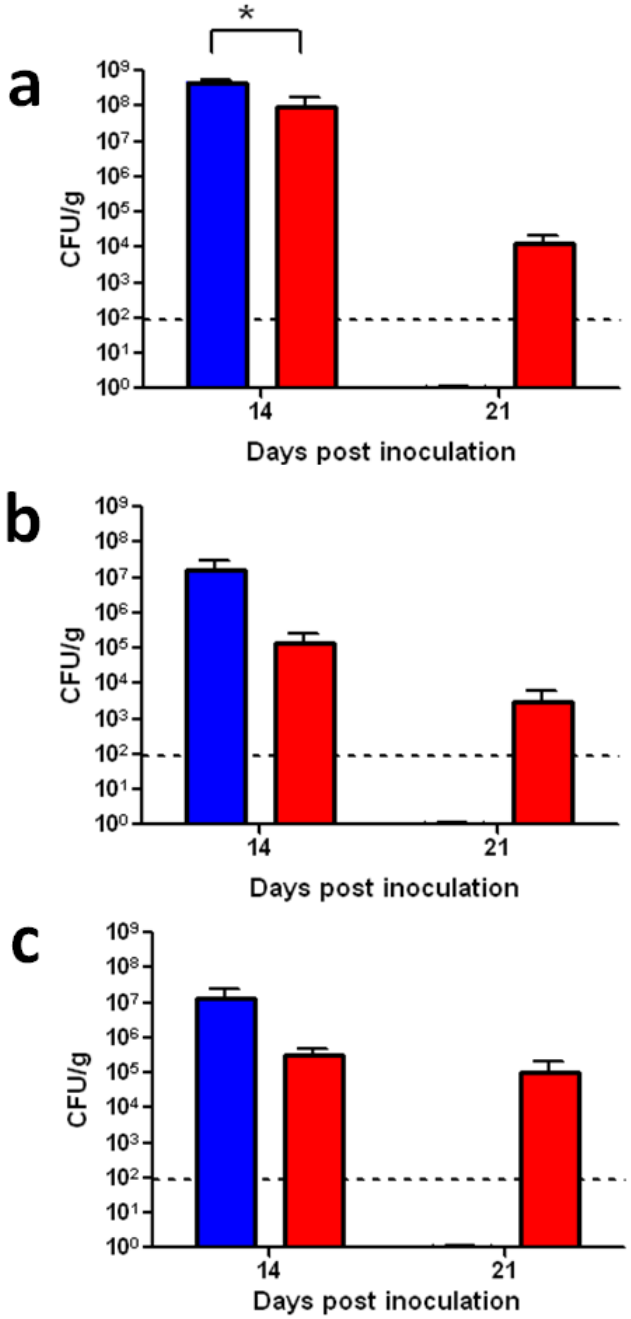

Figure 42. CFU of *C. rodentium* in gastrointestinal tissues of miR-155-deficient, µMT-deficient and control wild-type, µMT-deficient chimeras

Control wild-type, µMT-deficient (blue bars) and miR-155-deficient, µMT-deficient (red bars) mice were orally infected with 10^9 organisms of *C. rodentium.* On days 14 and 21 pi, mice were sacrificed and numbers of *C. rodentium* (±SEM) in gastrointestinal tissue; colon(a), caecum (b) and ceacal patch (c)were enumerated, n=2 and n=5 mice per group respectively, * indicates P value <0.0355 by students t test. Black broken lines indicate the detection level of the assay.

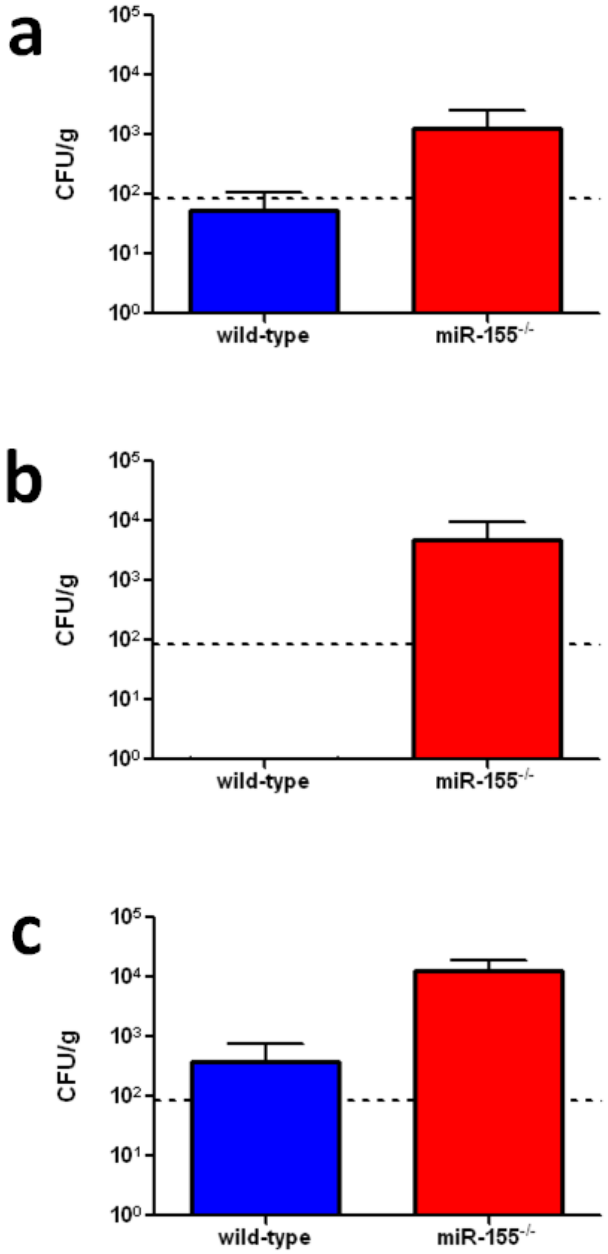

Figure 43. CFU of *C. rodentium* in systemic tissues of miR-155-deficient, µMT-deficient and control wild-type, µMT-deficient chimeras

Control wild-type, µMT-deficient (blue bars) and miR-155-deficient, µMT-deficient (red bars) mice were orally infected with 10^9 organisms of *C. rodentium.* On days 14, mice were sacrificed and numbers of *C. rodentium* (±SEM) in systemic tissues; spleen(a), liver (b) and mLNs (c)were enumerated, n=2 and n=5 mice per group respectively. Black broken lines indicate the detection level of the assay.

3.3.3 Absence of miR-155 leads to impaired production of *C. rodentium*-specific antibody

We also examined serum antibody responses against the *C. rodentium* surface-associated protein EspA in chimeric mice 14 days after challenge. Similar to the phenotype observed in miR-155-deficient mice, we found that there was a general trend towards reduced serum EspA-specific Ig and IgG production in chimeras with miR-155-deficient B cells compared to controls, although this was not statistically significant (Figure 44). It is worth noting that consistent with previously published work, we detected considerable amounts of EspA-specific Ig in one miR-155-deficient, μMT-deficient chimeric mouse perhaps, suggesting that some degree of antibody production is occurring[34]. However, this outlier could also have arisen either as a result of human or instrument error.

We were unable to detect EspA-specific IgG1 and IgG2a subclasses in either group of mice possibly because the levels are too small for our analysis.

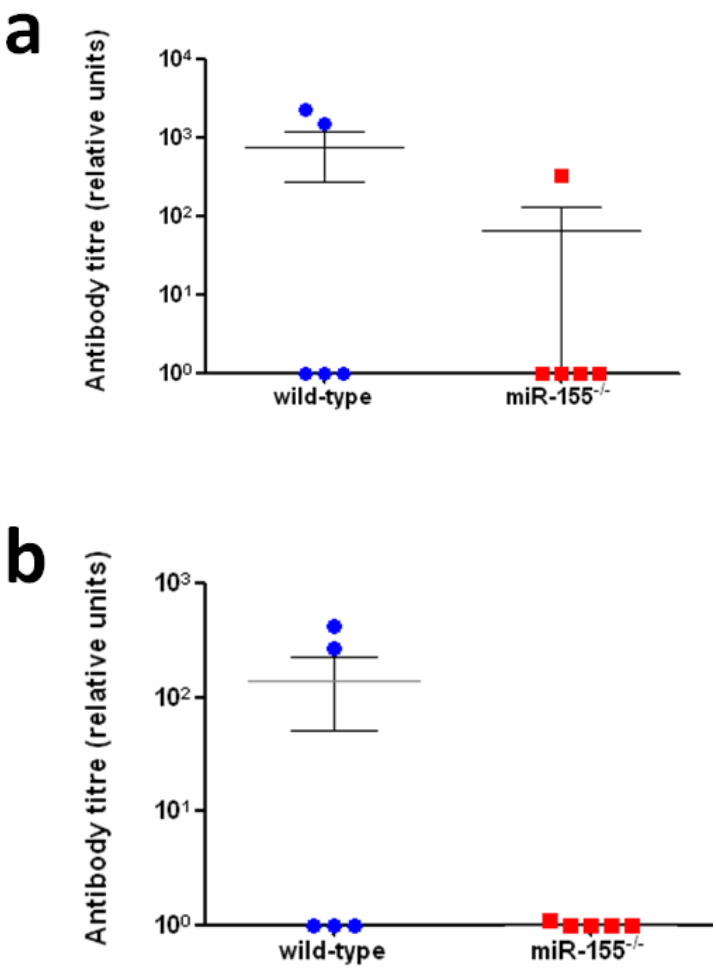

Figure 44. Humoral immune responses to *C. rodentium* surface protein EspA in miR-155-deficient, µMT-deficient and wild-type, µMT-deficient mice

Serum Ig (a) and IgG (b) antibody responses (± SEM) against the *C. rodentium* surface-associated protein EspA were determined in wild-type, µMT-deficient (blue circles) and miR-155-deficient, µMT-deficient (red squares) mice at 14 days pi with *C. rodentium*.

3.3.4 Impaired germinal centre formation is B cell intrinsic

Having found that miR-155-deficient, μMT-deficient chimeras produce very much reduced levels of EspA-specific antibody following challenge with *C. rodentium*, we further wished to determine whether this defect was accompanied by impaired germinal centre formation. We observed that miR-155-deficient, μMT-deficient chimeras displayed significantly fewer numbers of germinal centres in mLNs 21 days pi (Figure 45a, b and c). Additionally, the germinal centres produced were noticeably smaller than those of controls (Figure 45d). Together these results suggest that miR-155 plays an essential role in germinal centre formation and production of antigen-specific antibody in a B cell-autonomous manner.

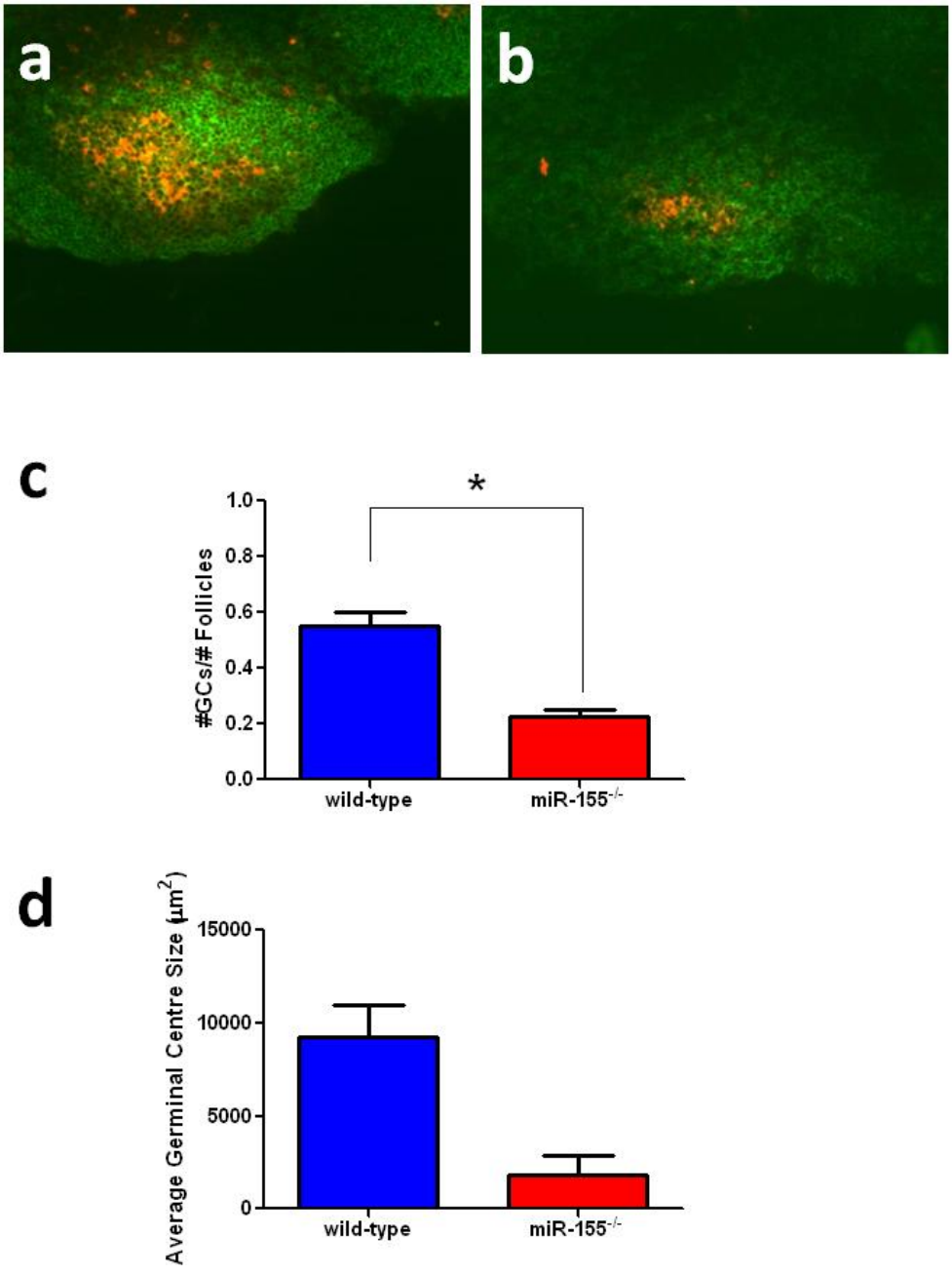

Figure 45. Germinal centre formation in miR-155-deficient, µMT-deficient and control wild-type, µMT-deficient mice, following infection with *C. rodentium*.

miR-155-deficient, µMT-deficient and control wild-type, µMT-deficient mice were infected orally with *C. rodentium* and germinal centre formation was analyzed 21 days pi. Immunohistochemistry was performed on mLNs from infected control wild-type, µMT-deficient (a), and infected miR-155-deficient, µMT-deficient (b) mice 21 days pi to detect germinal centres (Green, $B220^+$; Red/Orange, PNA^+), magnification x40. Number (c) and size (d) of GCs (±SEM) were determined from sections; n = 4 mice per group.

3.4 Discussion

The results of the current study provide valuable evidence for the importance of miR-155 in controlling infection with the mucosal pathogen, *C. rodentium*. We demonstrate that miR-155-deficient mice are highly susceptible to mucosal and even systemic infection with *C. rodentium*. We found that whilst colonisation in miR-155-deficient mice remained comparable with that observed in control mice throughout the early to middle phases of infection (4-14 days pi), during the later stages miR-155-deficient mice exhibited significantly greater pathogen burdens in all gastrointestinal tissues assayed. Furthermore, there was on average, a mean 20-day lag in resolution time of infection in miR-155-deficient mice. These data suggest that miR-155 is not obviously essential for the early innate control of bacteria but is critically important for acquired immune responses during the late bacterial clearance phase of infection.

The high and sustained pathogen load in the colons of *C. rodentium* infected miR-155-deficient mice was associated with the development of severe colonic pathology, in particular gross elongation of colonic crypts, polymorphonuclear infiltrate in the lamina propria and submucosa and frequent breaks in the epithelium integrity. We provide evidence that bacteria resident in the colon are able to translocate across the damaged epithelium and disseminate to internal tissues as indicated by the presence of significant numbers of *C. rodentium* in the spleens and livers of miR-155-deficient mice. Since it is known that systemic T cell-dependent antibody responses are critical for preventing bacteria spreading through the damaged mucosa, we hypothesised that the production of *C. rodentium*-specific antibody may be impaired in the absence of miR-155[170, 171, 208]. Subsequently, serum EspA-specific antibody responses were found to be significantly reduced in miR-155-deficient mice 14 and 45 days after infection. Furthermore, analysis of germinal centre formation in the mLNs and caecal patches of infected mice revealed that miR-155-deficient mice produce significantly fewer germinal centres than C57BL/6 mice. Genome-wide analysis of gene expression in *C.*

rodentium infected caecal patches provided indirect evidence that BCR signalling is significantly down-regulated in the absence of miR-155. This is consistent with a recently published report showing that miR-155 is rapidly expressed following cross-linking of the BCR and might explain why germinal centre development and the generation of plasma cells is severely impaired in mice lacking miR-155[23]. In addition, we found that the expression of chemokine receptor, CXCR3, was reduced in infected miR-155-deficient caecal patches. CXCR3 is known to be involved in the activation and chemotaxis of leukocytes as well as homing of murine-IgG-secreting plasma cells. Thus, it is likely that the down-regulation of CXCR3 is additionally likely to contribute to the defective germinal centre response observed in miR-155-deficient mice.

Having established that mice lacking miR-155 develop greatly increased tissue pathology following infection, we were somewhat surprised to find that there was very little difference in the overall colonic mRNA response to *C. rodentium* between infected miR-155-deficient and C57BL/6 mice. However, results from GO and KEGG conditional testing for overrepresentation and InnateDB analysis suggest that in the absence of miR-155 there is large scale dysregulation of numerous different immune response pathways, in addition to B cell mediated immunity, although the data did not reach significance. Specifically, all analyses identified that the T cell receptor signalling pathway was significantly associated with down-regulated genes. It is therefore likely that T cell function is also affected. Such a view is consistent with previously published reports that have shown that miR-155 is expressed in various different immune cells, including T and B lymphocytes, macrophages and dendritic cells following activation and plays an active role in their function[28, 29, 31, 33, 34].

It is worth noting that amongst the down-regulated genes in miR-155-deficient caecal patches and colons at both day 4 and 14 pi, there was an over-representation of genes involved in leukocyte migration and chemotaxis. For example, MMP3 was notably down-regulated in miR-155-deficient caecal patches, 4 days after infection. MMP3 is known to be involved in mediating

cell migration during tissue injury and is crucially important for the migration of $CD4^+$ T lymphocytes into the intestinal lamina propria during infection with *C. rodentium*. Based on these findings, we speculate that leukocyte trafficking may also be affected by the loss of miR-155 and may contribute to the susceptibility of miR-155-deficient mice. Though, further investigation would be needed to test this hypothesis, and this will be the next challenge.

It is apparent that B cell-mediated immune responses are central to the resolution of a *C. rodentium* infection and whilst ultimate eradication of infection depends on the production of pathogen-specific antibodies, it has been suggested that resistance to *C. rodentium* at the epithelium may additionally depend upon a population of $CD4^+$ T cells that produce proinflammatory cytokines which activate effector mechanisms at the epithelium[171]. Considering this and the fact that T cell-dependent B cell responses require reciprocal interactions between both B and T cells it was important for us to ascertain the relative contributions of miR-155-deficient T and B cells in pathogen-specific antibody responses. To address this, miR-155-deficient, μMT-deficient and wild-type, μMT-deficient chimeric mice were orally infected with 10^9 CFU of *C. rodentium*. Similar to that observed in miR-155-deficient germline mice, miR-155-deficient, μMT-deficient mice were highly susceptible to mucosal and systemic infection with *C. rodentium*. Chimeras with miR-155-deficient B cells took significantly longer to resolve infection than control chimeras and exhibited dramatically higher pathogen burdens in systemic and gastrointestinal tissues on days 14 and 21 after infection, respectively. Furthermore, miR-155-deficient, μMT-deficient mice had reduced serum EspA-specific Ig and IgG levels as a result of defective germinal centre formation. Collectively, these data imply that the susceptibility of miR-155-deficient mice and defective antibody responses is intrinsic to miR-155-deficient B cells. We observed that there was a slight amelioration in disease severity in chimeras possessing only miR-155-deficient B cells, compared with miR-155-deficient germline mice. miR-155-deficient, μMT-deficient chimeric mice infected with *C. rodentium* resolved infection within 4 weeks whereas germline mice took up to 6 weeks to

achieve complete clearance. The heightened susceptibility of miR-155-deficient germline mice could suggest that multiple different cells and signalling pathways are affected by the loss of miR-155. This corroborates our previous findings that B and T cell receptor signalling, chemotactic and leukocyte migration pathways are all significantly down-regulated in *C. rodentium* infected miR-155-deficient germline mice. Additionally, previous studies have also shown that miR-155-deficient mice exhibit defective B and T cell immunity as well as abnormal function of antigen-presenting cells[31, 33, 34].